Dalton Transactions

Accepted Manuscript

This is an *Accepted Manuscript*, which has been through the Royal Society of Chemistry peer review process and has been accepted for publication.

Accepted Manuscripts are published online shortly after acceptance, before technical editing, formatting and proof reading. Using this free service, authors can make their results available to the community, in citable form, before we publish the edited article. We will replace this *Accepted Manuscript* with the edited and formatted *Advance Article* as soon as it is available.

You can find more information about *Accepted Manuscripts* in the Information for Authors.

Please note that technical editing may introduce minor changes to the text and/or graphics, which may alter content. The journal's standard Terms & Conditions and the Ethical guidelines still apply. In no event shall the Royal Society of Chemistry be held responsible for any errors or omissions in this *Accepted Manuscript* or any consequences arising from the use of any information it contains.

ROYAL SOCIETY OF CHEMISTRY

www.rsc.org/dalton

A phosphomide based PNP ligand, 2,6-{$Ph_2PC(O)\}_2(C_5H_3N)$ showing PP, PNP and PNO coordination modes

Pawan Kumar,[a] Vitthalrao S. Kashid[a], Yernaidu Reddi[a], Joel T Mague[b], Raghavan B. Sunoj[a]* and Maravanji S. Balakrishna[a*]

[a]*Phosphorus Laboratory, Department of Chemistry, Indian Institute of Technology Bombay, Mumbai 400 076, India, and* [b]*Department of Chemistry, Tulane University, New Orleans, Louisiana 70118.*

A new class of PNP pincer ligand, pyridine-2,6-diylbis(diphenylphosphino)methanone, 2,6-{$Ph_2PC(O)\}_2(C_5H_3N)$ (**1**) (hereafter referred as "bis(phosphomide)") was prepared by the reaction of picolinoyldichloride with diphenylphosphine in the presence of triethylamine. The bis(phosphomide) **1** shows symmetrical PNP, unsymmetrical PNO and simple bidentate PP coordination modes when treated with various transition metal precursors. The reaction between **1** and [Ru(*p*-cymene)$Cl_2]_2$ in a 1:1 molar ratio yielded a binuclear complex [$Ru_2Cl_4(NCCH_3)$(*p*-cymene){2,6-{$Ph_2PC(O)\}_2(C_5H_3N)$}] (**2**) containing an unsymmetrical PNO pincer cage around one of the ruthenium centers, whereas the second ruthenium is bonded to the other phosphorus atom along with cymene and two chloride atoms. Symmetrical pincer complexes [$RuCl(NCCH_3)_2$ {2,6-{$Ph_2PC(O)\}_2(C_5H_3N)$}](ClO_4) (**3**), [Ru(η^5-C_5H_5){2,6-{$Ph_2PC(O)\}_2(C_5H_3N)$}](OTf) (**4**) and [RhCl{2,6-{$Ph_2PC(O)\}_2(C_5H_3N)$}] (**5**) were obtained in the respective reactions of **1** with [$RuCl(NCCH_3)_2$(*p*-cymene)](ClO_4), [Ru(η^5-C_5H_5)Cl(PPh_3)$_2$] and [Rh(COD)Cl]$_2$. Group 10 metal complexes [NiCl{2,6-{$Ph_2PC(O)\}_2(C_5H_3N)$}](BF_4) (**6**), [PdCl{2,6-{$Ph_2PC(O)\}_2(C_5H_3N)$}]ClO_4 (**7**) and [PtCl{2,6-{$Ph_2PC(O)\}_2(C_5H_3N)$}]ClO_4 (**8**) were

Dalton Transactions Accepted Manuscript

obtained by transmetallation reactions of *in situ* generated Ag^{I} salts of **1** with $Ni(DME)Cl_2$ or $M(COD)Cl_2$ (M = Ni, Pd and Pt). The reactions between **1** and CuX or $[Cu(NCCH_3)_4](BF_4)$ produced mononuclear complexes of the type $[CuX\{2,6\text{-}\{Ph_2PC(O)\}_2(C_5H_3N)\}]$ (**9**, X = Cl; **10**, X = Br; **11**, X = I), $[Cu(NCCH_3)\{Ph_2C(O)\}_2(C_5H_3N)\}](BF_4)$ (**12**) and $[Cu\{Ph_2C(O)\}_2(C_5H_3N)\}_2](BF_4)$ (**13**). Similarly, the silver complexes $[AgX\{2,6\text{-}\{Ph_2PC(O)\}_2(C_5H_3N)\}]$ (**14**, X = ClO_4; **15**, X = Br) were obtained by the treatment of **1** with $AgClO_4$ or AgBr in 1:1 molar ratios. Treatment of **1** with $AuCl(SMe_2)$ in 1:1 and 1:2 molar ratios produced mono- and binuclear complexes, $[AuCl\{2,6\text{-}\{Ph_2PC(O)\}_2(C_5H_3N)\}]$ (**16**) and $[Au_2Cl_2\{2,6\text{-}\{Ph_2PC(O)\}_2(C_5H_3N)\}]$ (**17**) in good yield. The structures of ligand **1** and complexes **2**, **5** and **17** were confirmed by single-crystal X-ray diffraction studies. DFT calculations were carried to gain more insight into the structure and bonding features as well as feasibility of some key chemical transformations.

Introduction

The last few decades have seen an enormous growth in the field of pincer ligands because of their importance in homogeneous catalysis and materials applications.[1] Transition metal complexes of these ligands catalyze a plethora of reactions ranging from organic transformations such as Aldol and Michael addition reactions[2] to olefin polymerization[3], alkane metathesis and alkane dehydrogenation.[4] Of the various types of pincer ligands described in the literature, phosphorus based ligands have attracted special attention as these allow fine tuning of steric and electronic properties around the metal center thereby making them efficient catalysts. The PNP type of pincer ligands with a central pyridine moiety show diverse reactivity pattern and have

Dalton Transactions Accepted Manuscript

been extensively used in coordination chemistry.[5] These are classified mainly into three types: PCNCP, POCOP and PN'NN'P, (N' = NR or NH) depending upon -CH_2-, -O- or -NR- linkers (Chart 1).[6] Milstein and coworkers and others have successfully employed the transition metal complexes of these ligands to activate C–H, C–C, O–H, N–H and S–H bonds[7] as well as small molecules like N_2, H_2 and CO_2.[8] The facile dearomatization of the pyridine ring by the deprotonation in the sidearm introduces metal-ligand cooperativity which is less likely in the PCP analogues due to high dearomatization energy. This non-innocent behavior and charge switching character of the pyridine based PNP pincer ligands plays an essential role in a number of catalytic transformations such as hydrogenation of esters, amides and CO_2,[9] dehydrogenative coupling and other related reactions.[10]

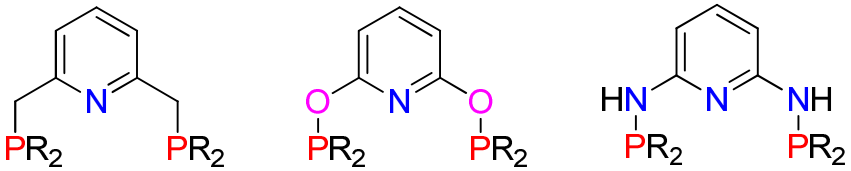

Chart 1

The synthesis and coordination chemistry of phosphomide based ligand system is scant which is mainly attributed to the sensitivity of the P–CO bond towards moisture and the difficulties involved in controlling their reactivity and isolation.[11] We have recently reported the synthesis of bisphosphomide ligand [1,3-{$Ph_2PC(O)$}$_2$(C_6H_4)] and studied its coordination behavior in detail.[6] The PCP pincer complexes of these ligands have been synthesized *via* C–H bond activation as well as by oxidative addition of the prefunctionalized ligand with zero-valent metal precursors. We envisioned that the similar carbonyl-linked PNP ligand system would be even more interesting since the presence of both phosphorus and oxygen donor atoms could

Dalton Transactions Accepted Manuscript

enable it to adopt variable coordination modes. As a continuation of our interest in designing new inexpensive ligands and studying their coordination behavior and catalytic applications[13] we report the synthesis of a pyridine-based bisphosphomide ligand and its transition metal chemistry.

Results and discussion

Synthesis of bisphosphomide ligand 2,6-$\{Ph_2PC(O)\}_2(C_5H_3N)$ (1)

The reaction of picolinoyldichloride with two equivalents of diphenylphosphine in the presence of triethylamine at 0 °C afforded the tridentate PNP ligand 2,6-$\{Ph_2PC(O)\}_2(C_5H_3N)$ (**1**) in quantitative yield (Scheme 1). The ligand **1** is a low-melting orange-yellow solid with moderate stability towards air and moisture.

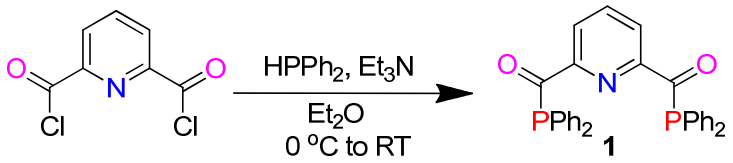

Scheme 1

The $^{31}P\{^1H\}$ NMR spectrum of **1** displays a single resonance at 17.5 ppm which is slightly deshielded in comparison with the corresponding PCP analogue (12.5 ppm) and is attributed to the electron withdrawing nature of the pyridine ring. In the ^1H NMR spectrum, the pyridine protons appear as a broad singlet at 7.84 ppm. The IR spectrum of **1** exhibits a strong ν_{CO} band at 1656 cm^{-1}. The structure of ligand **1** was further confirmed by a single crystal X-ray structure determination. The molecular structure of **1** depicts that both the donor arms of bisphosphomide ligand are almost coplanar with the pyridine ring (Fig. 1). The distance between the two phosphorus atoms (P···P) is 4.429 Å while the distance between two carbonyl carbon atoms is

Dalton Transactions Accepted Manuscript

4.818 Å. The C—O and P—CO distances in **1** are 1.21 and 1.86 Å whereas the P1–C13–C14 and P2–C18–C19 bond angles are 115.20(10)^{o} and 116.83(9)^{o}, respectively.

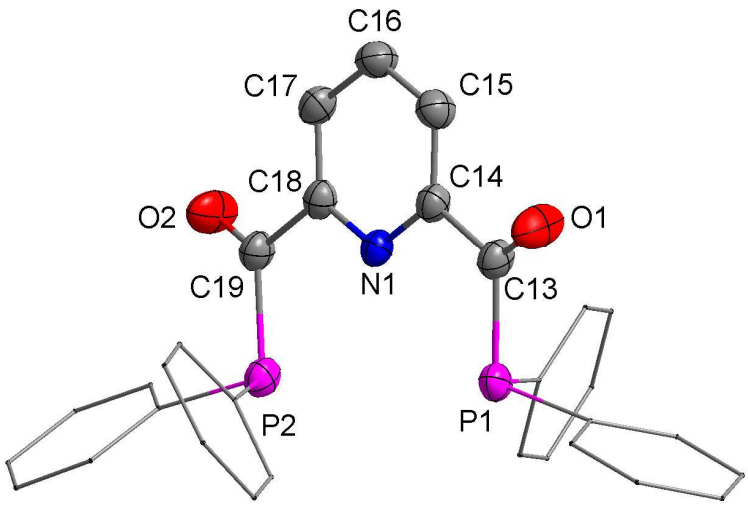

Fig. 1 Molecular structure of ligand, 2,6-{$Ph_2PC(O)$}$_2$(C_5H_3N) (**1**). All hydrogen atoms have been omitted for clarity. Thermal ellipsoids are drawn at the 50% probability level.

Compound **1** is essentially a trifunctional ligand with a combination of two soft phosphorus atoms, two oxygen atoms and a pyridyl N atom. Due to this, the coordination behavior of this ligand is interesting since the free rotation of donor arms can give a possible combination of PNP, ONO or PNO coordination modes. The choice of the metal ions/atoms can also influence the different coordinating modes.

Various possible coordination modes, as depicted in Chart 2, can be observed upon reacting **1** with transition metal precursors. Bidentate chelation of **1** to the metal center can be either symmetrical PP or OO or a hybrid OP coordination, whereas the tridentate coordination can lead to the formation of symmetrical PNP or ONO complex or a hybrid PNO complex. The transition

Dalton Transactions Accepted Manuscript

metal chemistry of this multi-functional ligand **1** was carried out in order to understand its coordination behavior.

In order to gain additional insights into the coordination properties of bisphosphomide ligand **1**, density functional theory computations were performed using the M06 and B3LYP functionals (with 6-31G** basis set for C, H, O, N, P and Cl and SDD for heavier metals Rh, Ru and Au). A comparison of the computed geometric parameters with that obtained through X-ray crystallography for the free pincer ligand is provided in Table 2.[14] The structural parameters showed generally good agreement.

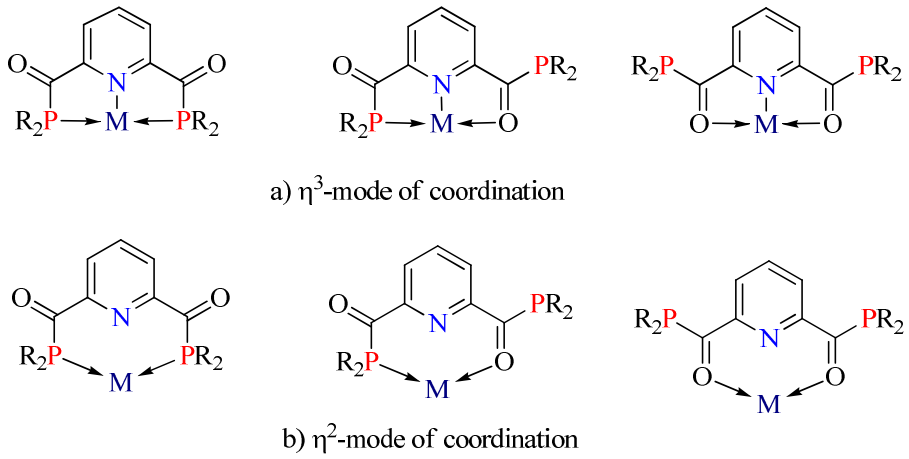

Chart 2 Possible coordinating modes of ligand **1**

Ruthenium(II) and Rhodium(I) complexes

The reaction of **1** with $[Ru(p\text{-cymene})Cl_2]_2$ in a 1:1 molar ratio at room temperature afforded a binuclear complex, $[Ru_2Cl_4(NCCH_3)(p\text{-cymene})\{2,6\text{-}\{Ph_2PC(O)\}_2(C_5H_3N)\}]$ (**2**) in 72% yield. One of the ruthenium centers is coordinated *via* the PNO mode whereas the other ruthenium is bonded to a phosphorus atom, two chlorine atoms and a η^6-cymene ligand as shown in Scheme 2. Similar reaction of the bis(phosphomide) ligand, $1,3\text{-}\{Ph_2PC(O)\}_2(C_6H_4)$, reported by our group recently, yielded a binuclear complex (**I**) of the type **2a** showing two phosphorus arms independently coordinating to $[Ru(\eta^6\text{-cymene})Cl_2]$ moieties with one of the ruthenium atoms

Dalton Transactions Accepted Manuscript

being closer to the pincer carbon atom at a bond distance of 3.311 Å. It is anticipated that such short distances can facilitate bonding interactions through the interemediates **2a** and **2b** thus facilitating the PNO pincer formation which requires simply the free rotation of the other ruthenium bound phosphorus arm to bring the carbonyl group closer to the metal center.

The reactions between [Ru(η^6-cymene)Cl_2] and **1** or its PCP analog are facile as can be seen from the computed ΔG values for the formation of **2a** (ΔG = -15.6 kcal/mol) and **I** (ΔG = -15.87 kcal/mol). Transformation of **2a** to **2b** (ΔG = -22.9 kcal/mol) and eventually to **2** (ΔG = -43.9 kcal/mol) are very facile due to the close proximity of pyridyl lone pair to the ruthenium center. Such transformation are less likely in the case of **I** as C–H activation requires drastic and prolonged reaction conitions.

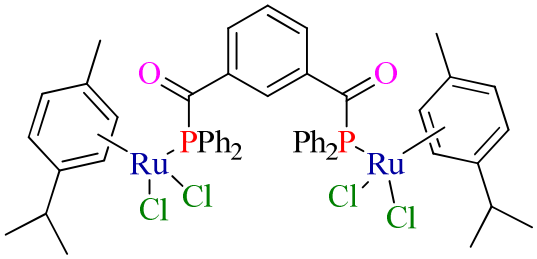

I

The $^{31}P\{^1H\}$ NMR spectrum of **2** shows two doublets centered at 28.3 and 79.5 ppm with a $^4J_{PP}$ coupling of 6.5 Hz indicating the presence of two different types of phosphorus centers. The chemical shift at 79.5 ppm was assigned to phosphorus center involved in PNO coordination, whereas the upfield signal at 29.5 ppm was due to the other phosphorus atom. The ^1H NMR integration supports the presence of one cymene group in the molecule with two doublets centered at 5.63 and 5.47 ($^3J_{HH}$ = 5.5 Hz), the characteristic doublet and septet pattern for the isopropyl group was observed at 0.97 and 2.61 ppm and a singlet at 1.67 ppm for methyl group.

Dalton Transactions Accepted Manuscript

The central pyridine ring displays two doublets centered at 8.51 and 7.74 ppm corresponding to the protons *ortho* to the coordinated and uncoordinated carbonyl groups. There are some examples of PNO types of ligands described in literature, but with very different frameworks.[15]

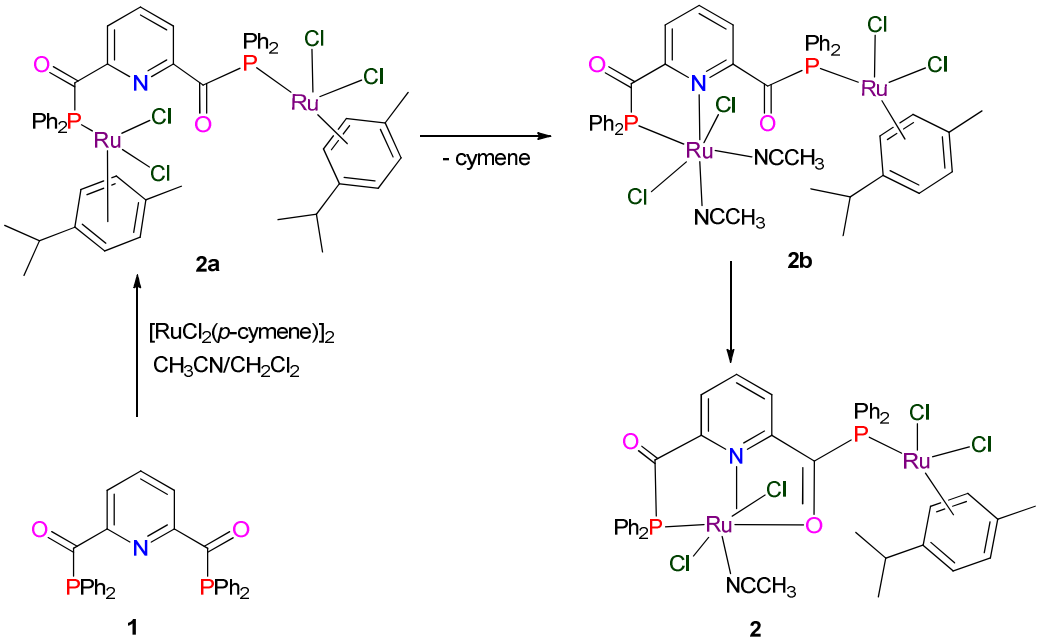

Scheme 2

The molecular structure of complex **2** is further confirmed by a single crystal X-ray diffraction study. The molecular structure consists of two ruthenium(II) centers coordinated in κ^3PNO, κ^1P bonding modes. One of the ruthenium(II) atoms is coordinated in a terdentate PNO pincer fashion whereas the other ruthenium is surrounded by one phosphorus, with two chlorides and a cymene group (Fig. 2). The geometry around Ru1 is octahedral, whereas Ru2 is pseudo octahedral. The Ru1–P1 [2.2260(8) Å] bond distance is slightly shorter than that of Ru2–P2 [2.3486(9) Å] and the Ru1–O2 bond distance is 2.146(2) Å. One of the five membered chelate rings, formed because of P coordination, is larger in size and is exactly in the plane of the pyridine backbone with a C13–P1–Ru1 bond angle of 99.25(10)°. The other chelate ring is

Dalton Transactions Accepted Manuscript

slightly out of the plane of the pyridine ring with a C19–O2–Ru1 bond angle of 113.12(19)^{o}. The P1–C13 [1.896(3) Å] bond distance is slightly larger than that of P2–C19 [1.860(3) Å] whereas the O1–C13[1.211(4) Å] bond distance is slightly shorter than that of O2–C19[1.237(4) Å]. The Ru–C bond distances range from 2.179(3) to 2.242(3) Å with an average bond distance of 2.216 Å. The bond angle Cl3–Ru2–Cl4 is 87.69(3)^{o} which compares well with the reported range of Cl–Ru–Cl bond angles (86.27-89.77^{o}) for [Ru(*p*-cymene)Cl_2(L)] type complexes.[16]

The calculated relative Gibbs free energies (at the M06/6-31G**, SDD level of theory) with respect to the separated reactants (**1**, [Ru(η^6-cymene)Cl_2]$_2$ and CH_3CN) for complexes **2a** and **2b** (Scheme 2), which are found to be -15.5 and -22.8 kcal/mol, indicate that complex **2b** enjoys an additional stabilization compared to complex **2a**. More importantly, the formation of **2** is found to be exergonic by 44 kcal/mol, which is in line with the experimental observation and characterization of **2**.

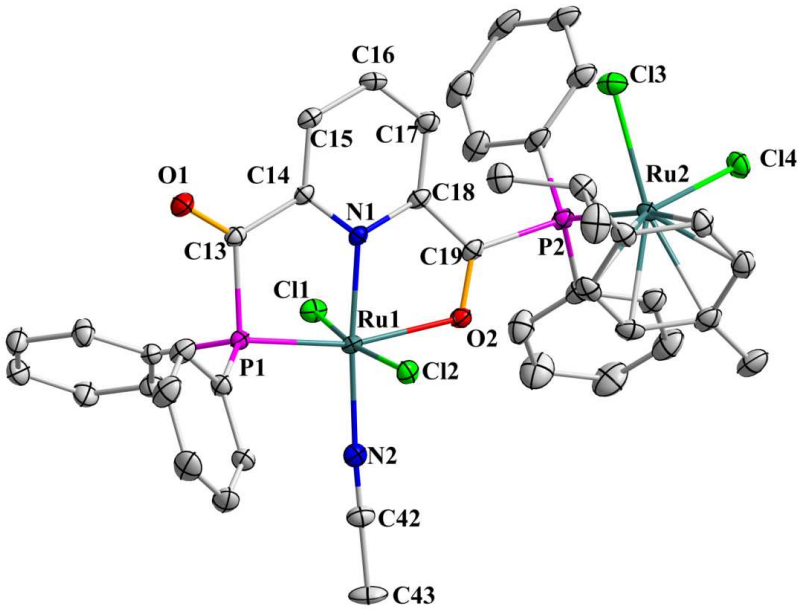

Fig. 2. Molecular structure of [Ru_2Cl_4($NCCH_3$)(*p*-cymene){2,6-{$Ph_2PC(O)$}$_2$(C_5H_3N)}] (**2**). All hydrogen atoms have been omitted for clarity. Thermal ellipsoids are drawn at the 50% probability level.

Dalton Transactions Accepted Manuscript

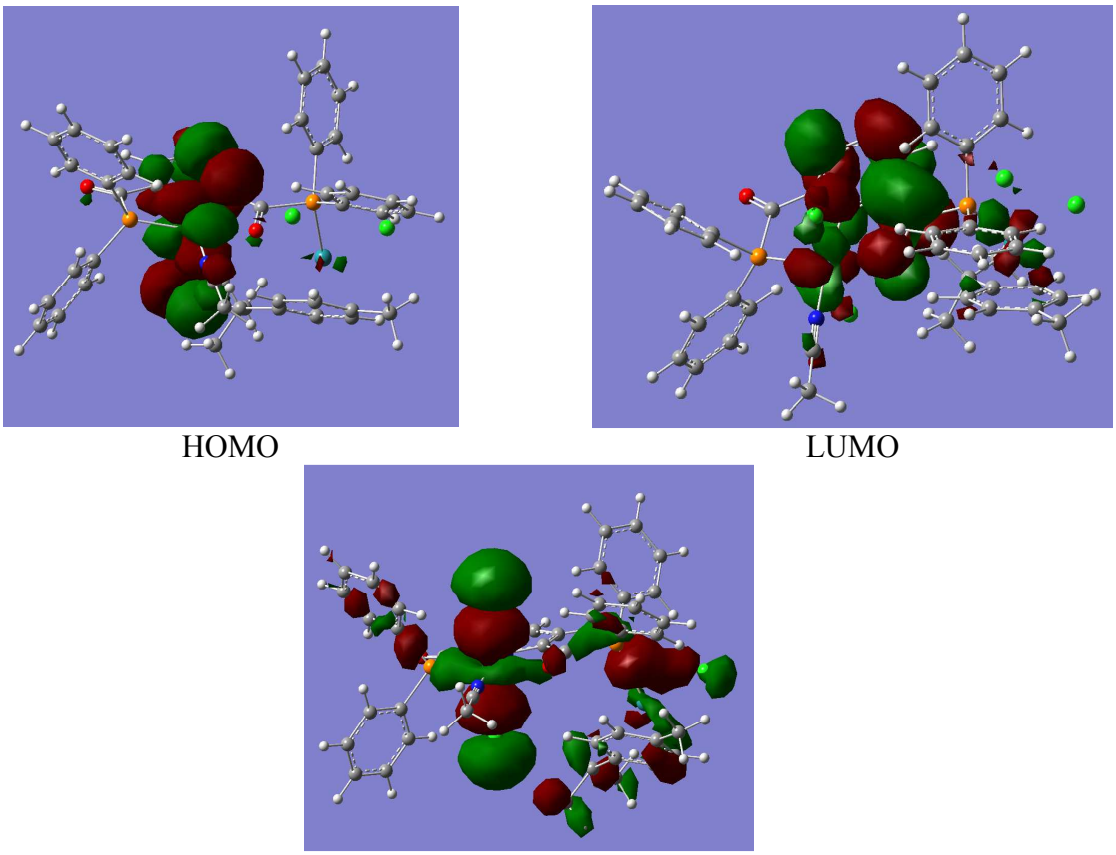

Fig. 3. Selected set of Kohn–Sham orbital contours for key orbitals of the Ru-PNO pincer complex **2**.

We have performed an AOMix analysis for ruthenium pincer PNO complex **2** using the B3LYP/6-31G**, SDD level of theory. In this method, the important Kohn-Sham orbitals are analyzed for its constituent atomic orbital contribution from different fragments in the molecule.[17] We focus on two key fragments, namely [Ru(**1**)Cl_2($NCCH_3$)] and the rest of the molecule considered as a ligand bound to the first fragment (See Fig. S1 in the Supporting Information). The orbital compositions are summarized in Table 1.

The HOMO of ruthenium complex **2** is identified as a primarily Ru(1) centered orbital (~90%). The LUMO consists of the PNO ligand and the Ru(2) center with only little contribution from Ru(1). In the case of HOMO-29, as shown in Fig. 3, Ru(1) interacts with the carbonyl

Dalton Transactions Accepted Manuscript

oxygen as well as with the phosphorus of the PNO ligand. The percentage composition of Ru(1) is about 80% and the remaining 20% is a combination of pincer ligand and Ru(2) as shown in Table 1. These orbitals indicate the donor-acceptor interactions between Ru(1) and carbonyl oxygen of the PNP ligand. The charge decomposition analysis further reveals that the charge donation from [$RuCl_2$(*p*-cymene){2,6-{$Ph_2PC(O)$}$_2$(C_5H_3N)}] to [$RuCl_2(NCCH_3)$] is 0.211 electrons where as back donation from Ru(1) center-to-combination of PNP and Ru(2) center is found to be 0.257 electrons.

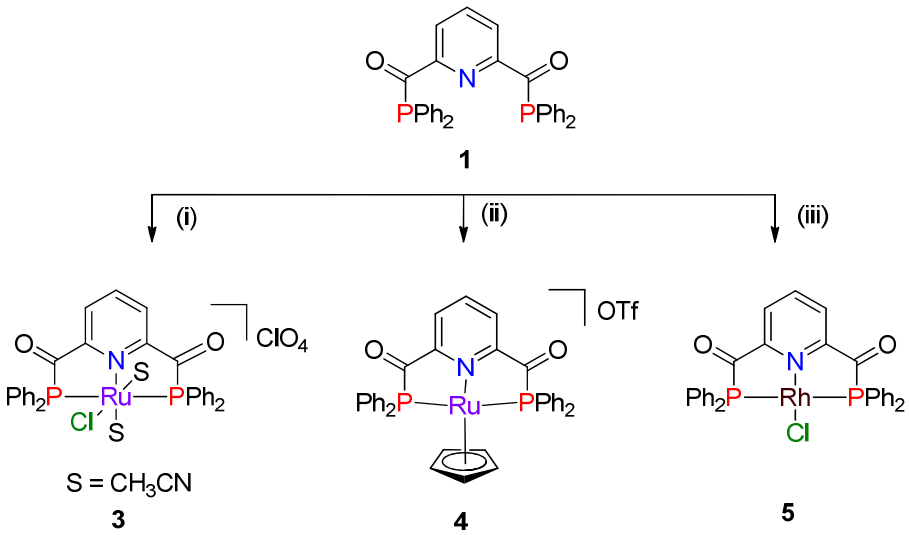

Scheme 3 (i) [$RuCl(NCCH_3)_2$(*p*-cymene)](ClO_4), CH_3CN; (ii) [Ru(η^5-C_5H_5)Cl(PPh_3)$_2$], AgOTf, CH_3CN; (iii) 0.5 [RhCl(COD)]$_2$, CH_2Cl_2.

Attempts to obtain a symmetrical Ru(κ^3-PNP) complex by the reaction of **1** with half an equivalent of [$RuCl_2$(*p*-Cymene)]$_2$ have been unsuccessful and resulted in the formation of a mixture of products containing **2** as major product along with some unidentified species. However, the reaction of **1** with *in situ* generated [$RuCl(NCCH_3)_2$(*p*-cymene)](ClO_4) exclusively afforded the desired complex [$RuCl(NCCH_3)_2$ {2,6-{$Ph_2PC(O)$}$_2$(C_5H_3N)-κ^3*PNP*}] (**3**) as dark brown solid (Scheme 3). Similarly, treatment of **1** with [Ru(η^5-C_5H_5)(PPh_3)$_2$](OTf) in 1:1 molar ratio afforded the [Ru(η^5-C_5H_5){2,6-{$Ph_2PC(O)$}$_2$(C_5H_3N)}](OTf) (**4**) as yellow solid. The reaction of **1** with [Rh(COD)Cl]$_2$ in a 2:1 molar ratio afforded the [RhCl{2,6-

Dalton Transactions Accepted Manuscript

$\{Ph_2PC(O)\}_2(C_5H_3N)\}$] (**5**) as brown solid. The $^{31}P\{^1H\}$ NMR spectra of complexes **3-5** exhibit a single resonances at 51.9, 42.3 and 37.6 ppm, respectively, with rhodium complex **5** showing $^1J_{RhP}$ coupling of 104.3 Hz. The structure of **5** has been confirmed by single crystal X-ray analysis. As depicted in the molecular structure of **5**, the ligand is coordinated to rhodium metal in a typical *mer*-κ^3-PNP fashion (Fig. 4). Similar to the known rhodium pincer complexes[18] the phosphorus atoms are located above the plane of pyridine ring in the same side resulting in a distorted square planar geometry around rhodium with P1–Rh–P2 bond angle of 153.10(22)^o. The two five membered fused rings are puckered with an N–Rh–Cl bond angle of 176.71(4)^o. The P1–C13–C14 and P2–C19–C18 bond angles are 112.07(12) and 113.19(12)^o which are slightly less than the same bond angles in **1** [115.20(10) and 116.83(9)^o]. The Rh–N [2.0375(14) Å], Rh–P1 [2.2523(6) Å] and Rh–P2 [2.2611(6) Å] bond distances are in the range of typical bond distances reported for PNP-Rh complexes.[18] The C13–O1 and C19–O2 bond distances are 1.209(2) and 1.211(2) Å.

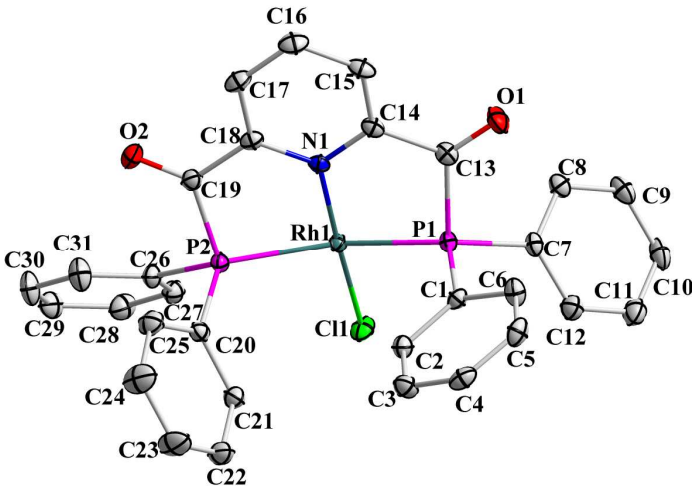

Fig. 4. Molecular structure of [RhCl{2,6-$\{Ph_2PC(O)\}_2(C_5H_3N)\}$] (**5**). All hydrogen atoms have been omitted for clarity. Thermal ellipsoids are drawn at the 50% probability level.

Dalton Transactions Accepted Manuscript

Group 10 metal PNP pincer complexes

The direct reaction between **1** and [Ni(DME)Cl_2] or M(COD)Cl_2 (M = Pd, Pt and Ni) in the presence of one equivalent of $AgClO_4$ or $AgBF_4$ resulted in the formation PNP–M complexes [MCl{2,6-{$Ph_2PC(O)$}$_2$(C_5H_3N)}]ClO_4 (**6**, M = Ni; **7**, M = Pd; **8**, M = Pt). Slow diffusion of diethyl ether into the dichloromethane solution of complexes **6**, **7** and **8** gave brown, yellow and greenish-yellow crystalline solids in 90%, 73% and 69% yields, respectively. The $^{31}P\{^1H\}$ NMR spectrum of nickel and palladium complexes **6** and **7** showed single resonances at 28.7 and 45.1 ppm which is slightly shielded in comparison to the PCP analogue (49.3 ppm)[12] while the platinum complex **8** also displayed a single resonance at 32.9 ppm with characteristic satellite peaks showing $^1J_{PtP}$ coupling of 2733 Hz. The IR spectra of **6**, **7** and **8** exhibit strong ν_{CO} absorption bands at 1685, 1695 and 1678 cm^{-1}. The structures and molecular compositions of these complexes were further confirmed by ^1H NMR and microanalytical data.

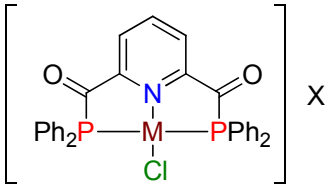

6 M = Ni, X = BF_4
7 M = Pd, X = ClO_4
8 M = Pt, X = ClO_4

Group 11 metal complexes

In comparison with other transition metals, the group 11 metal chemistry of PNP ligands has attracted less attention and has been recently examined by van der Vlugt and co-workers.[19] They observed that the presence of bulky substituents on phosphorus plays a decisive role in the formation of N-coordinated CuBr complexes. However, replacement of halides with bulky anions produced the N-coordinated cationic T-shaped Cu^I complexes in all cases (Chart 3).[19b]

Dalton Transactions Accepted Manuscript

The reactions between **1** and CuX (CuX, X = I, Br, Cl) or $[Cu(NCCH_3)_4](BF_4)$ in dichloromethane/acetonitrile produced mononuclear complexes of type $[CuX\{2,6\text{-}\{Ph_2PC(O)\}_2(C_5H_3N)\}]$ (**9**, X = Cl; **10**, X = Br; **11**, X = I), $[Cu(NCCH_3)\{2,6\text{-}\{Ph_2PC(O)\}_2(C_5H_3N)\}](BF_4)$ (**12**), and $[Cu\{2,6\text{-}\{Ph_2PC(O)\}_2(C_5H_3N)\}_2](BF_4)$ (**13**) as shown in Scheme 4. The $^{31}P\{^1H\}$ NMR spectra of complexes **9 - 13** showed single resonances in the range 0.1 to 6.0 ppm. In PNP^{tBu} and PNP^{Ph} complexes, N-coordination to metal was confirmed by the presence of two characteristic absorption bands around 1568 and 1603 cm^{-1}.[20,21] In the IR spectra of **9-11**, strong absorptions were observed for carbonyl groups (1677-1683 cm^{-1}) and ring vibrations of pyridine (1430-1436 cm^{-1}) but the characteristic pattern for N-coordination was absent confirming the formation of tricoordinated Cu^I complexes where the ligand exhibits bidentate (P,P) coordination mode.

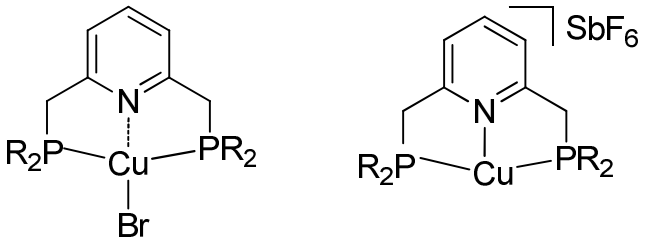

Chart 3

Treatment of **1** with AgX (X = ClO_4, Br) in 1:1 molar ratio provided the mononuclear complexes, $[AgX\{2,6\text{-}\{Ph_2PC(O)\}_2(C_5H_3N)\}]$ (**14**, X = ClO_4; **15**, X = Br) in good yields. The $^{31}P\{^1H\}$ NMR spectra of complexes **14** and **15** showed single broad resonances at 4.9 and 5.6 ppm. The presence of the molecular ion peak (m/z) at 708.9 confirmed the molecular structure of **14**, whereas in the mass spectrum of **15**, a (M^+-Br) peak was observed at m/z 610.1. The reaction of **1** with $[AuCl(SMe_2)]$ in 1:1 molar ratio resulted in the formation of a mononuclear complex,

Dalton Transactions Accepted Manuscript

[AuCl{2,6-{$Ph_2PC(O)$}$_2$(C_5H_3N)}] (**16**). Similar reaction of **1** with two equivalents of [AuCl(SMe_2)] afforded the binuclear complex, [Au_2Cl_2\{2,6-{$Ph_2PC(O)$}$_2$(C_5H_3N)}] (**17**). The $^{31}P\{^1H\}$ NMR spectra of complexes **16** and **17** exhibit single resonances at 24.6 and 38.5 ppm, respectively. In the mass spectrum of complex **16**, a peak at 700.1 was observed for the ion corresponding to (M^+-Cl).

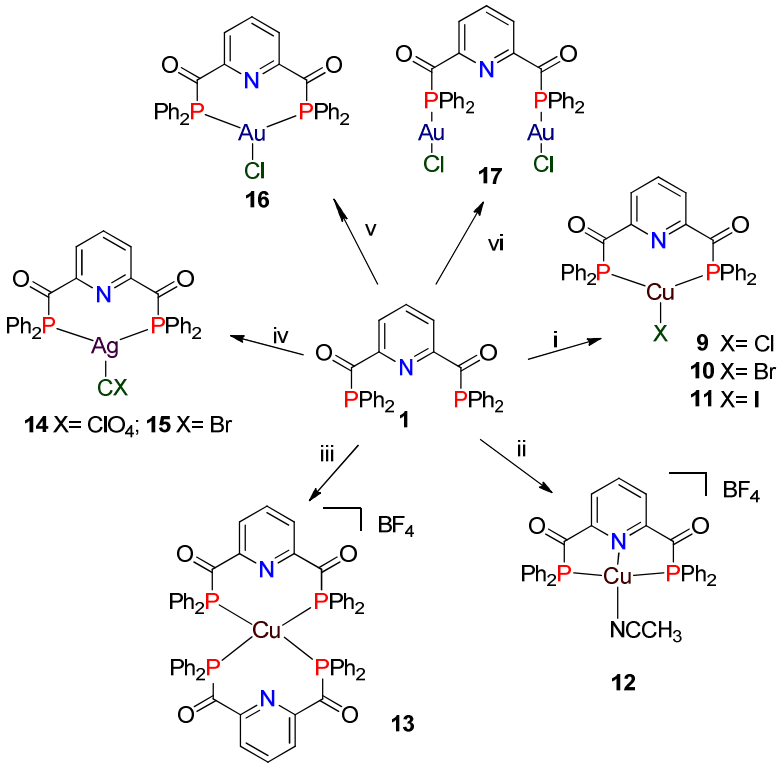

Scheme 4 (i) CuX, CH_2Cl_2/CH_3CN; (ii) [$Cu(CH_3CN)_4$]BF_4, CH_3CN; (iii) 0.5 [$Cu(CH_3CN)_4$]BF_4, CH_3CN; (iv) AgX, THF; (v) AuCl(SMe_2), CH_2Cl_2; (vi) 2 AuCl(SMe_2), CH_2Cl_2

The molecular structure of **17** was confirmed by a single crystal X-ray diffraction study. Complex **17** is a binuclear complex where each Au^I center displays linear geometry with bond angles P1–Au1–Cl2 and P2–Au2–Cl1 of 167.58(4)^o and 173.52(4)^o, (Fig. 6). The bond angles for C13–P1–Au1 and C19–P2–Au2 are 117.14(13)^o and 110.45(14)^o, respectively. The bond lengths of C13–O1 and C19–O2 are 1.203(5) Å and 1.212(5) Å, respectively. Both the values are very close to that observed for the ligand [C13–O1 = 1.2114(17) and C19–O2 = 1.2108(17) Å] which

Dalton Transactions Accepted Manuscript

indicates that the coordination of the lone pair of electrons on phosphorus does not have any effect on the C=O bond strength as predicted by theoretical calculation.[22] The P1–C13 (1.881(4) Å) and P2–C19 (1.893(4) Å) bond lengths are slightly longer than the same in the free ligand (1.8195 and 1.8242 Å). The structure shows the presence of an intramolecular aurophilic interaction with Au···Au distance of 3.1445(7) Å, which is less than the sum of the van der Waals' radii (3.6 Å).

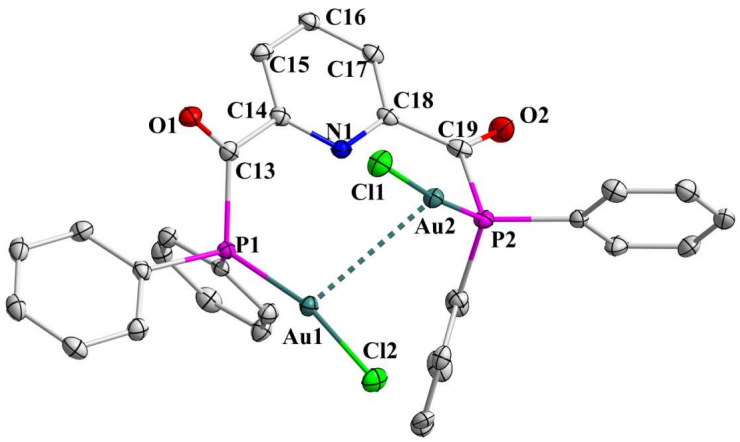

Fig. 6. Molecular structure of complex, $[Au_2Cl_2\{2,6\text{-}\{Ph_2PC(O)\}_2(C_5H_3N)\}]$ (**17**). All hydrogen atoms have been omitted for clarity. Thermal ellipsoids are drawn at the 50% probability level.

The interesting contact distance between the gold atoms in **17** prompted us to examine the bonding in this compound in greater detail. The geometry of the digold complex **17** was first optimized at the M06/6-31G**,SDD level of theory. The computed geometric parameters showed a generally good agreement, including that of the Au-Au atom distance, with the X-ray crystallographic data (Fig. 6/Table 2). Subsequently, an atoms-in-molecules (AIM) analysis for a bimetallic gold PNP complex was carried out using the B3LYP/6-31G**, SDD level of theory. Interestingly, the AIM analysis showed a distinct bond critical point between two gold atoms as

Dalton Transactions Accepted Manuscript

shown by the red dot in Fig. 7. It reveals the presence of an interaction between the two gold atoms in complex **17**.

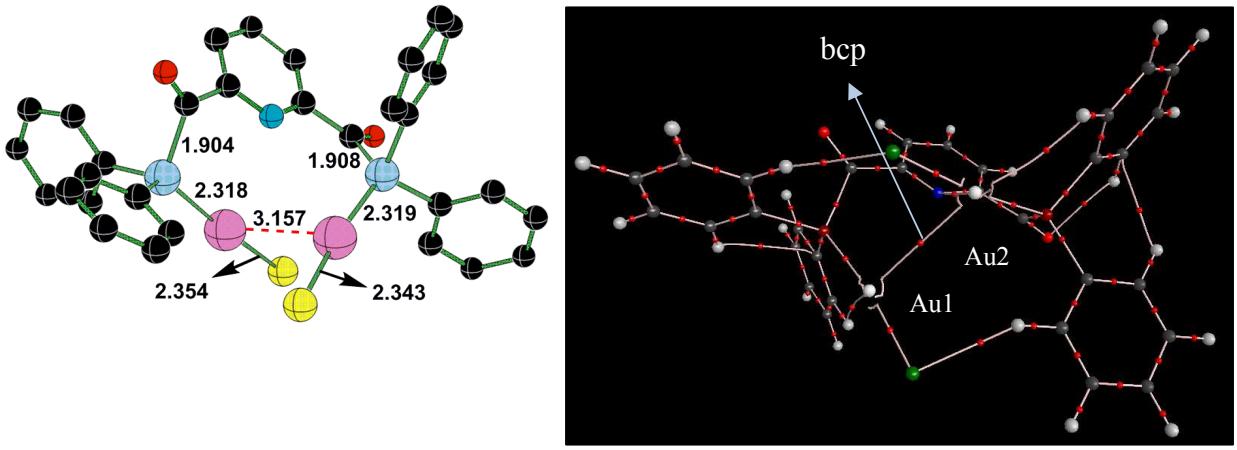

Fig. 7. Topological map showing bond paths and bond critical points in gold PNP pincer complex **17**.

Conclusions

Synthesis of a novel bisphosphomide PNP ligand and its low-valent late metal complexes are reported. The presence of three types of donor sites makes the ligand interesting and enables it to switch to different coordination modes. Symmetrical PNP–M complexes were obtained in the reaction of ligand **1** with Rh^{I}, Pd^{II}, Pt^{II}, Ni^{II} and Cu^{I} metal precursors. Both symmetrical (PNP–M) as well as unsymmetrical (PNO–M) coordination modes were observed in the case of Ru^{II} complexes. With group 11 metal precursors (Cu^{I}, Ag^{I} and Au^{I}) simple PP bidentate mode of coordination was observed. Although the utility of pincer complexes in catalytic applications is growing rapidly, mechanistic aspects are not too clear although it is presumed that the pincer framework remains intact during the catalytic process. The modified approach to incorporate a hard donor site to a typical low valent metal along with soft P enhances the possibility of the

Dalton Transactions Accepted Manuscript

reversible dissociation of M–L (hard) during oxidative addition thus bringing a new dimension to their versatile catalytic abilities in various organic transformations. Thus the bisphosphomide ligand **1** exhibits variable coordination behavior which is rarely observed in pincer type frameworks. Further synthesis of heterobimetallic complexes and catalytic studies of this class of ligands are in progress in our laboratory.

Experimental

General Procedures

All manipulations were performed using standard vacuum-line and Schlenk techniques under nitrogen atmosphere unless otherwise stated. All of the solvents were purified by conventional procedures[23] and distilled prior to use. The compounds CuCl, CuBr,[24], $[Cu(NCCH_3)_4](BF_4)$,[25] $AuCl(SMe_2)$,[26] $[Ru(\eta^6\text{-}p\text{-cymene})Cl_2]_2$,[27] $[Rh(COD)Cl]_2$,[28] $[Ru(\eta^5\text{-}C_5H_5)Cl(PPh_3)_2]$ and $M(COD)Cl_2$, (M = Pd, Pt)[29] were prepared according to the published procedures. The metal precursors CuI, AgBr and $AgClO_4$ were purchased from Aldrich chemicals and used as received. Other chemicals were obtained from commercial sources and purified prior to use.

Instrumentation

The NMR spectra were recorded at the following frequencies: 300 MHz (^{1}H), 121 MHz (^{31}P), 400 MHz (^{1}H), 100 MHz (^{13}C), 162 MHz (^{31}P) using Varian VXR 300 or Varian VXR 400 or Bruker AV 400 spectrometers. $^{13}C\{^1H\}$ and $^{31}P\{^1H\}$ NMR spectra were acquired using broad band decoupling. The spectra were recorded in $CDCl_3$ solutions with $CDCl_3$ as an internal lock; chemical shifts of ^{1}H and ^{13}C NMR spectra are reported in ppm downfield from TMS, used as an internal standard. The chemical shifts of $^{31}P\{^1H\}$ NMR spectra are referred to 85% H_3PO_4 as external standard. The microanalyses were performed using a Carlo Erba Model 1112 elemental

Dalton Transactions Accepted Manuscript

analyzer. Mass spectra were recorded using Waters Q-Tof micro (YA-105). The melting points were observed in capillary tubes and are uncorrected.

Synthesis of [2,6-{$Ph_2PC(O)$}$_2$(C_5H_3N)] (1)

To a solution of diphenylphosphine (5.5g, 29.4 mmol) in diethyl ether (40 mL) was added dropwise a solution of picolinoyl dichloride (3.0 g, 14.7 mmol) in 15 mL diethyl ether over 10 minutes at 0 ^oC in the presence of Et_3N (2.9 g, 4.0 mL, 29.4 mmol) during which the color of the solution turned to orange-yellow. The reaction mixture was stirred for 4 h at room temperature and the amine hydrochloride was removed by filtration. The solution was dried under reduced pressure and the residue redissolved in CH_2Cl_2 (65 mL) followed by saturation with 12 mL of petroleum ether to give light orange-yellow crystals of **1**. Yield: 95% (7.0 g). Mp: 173–175 °C. Anal. Calcd. for $C_{31}H_{23}NO_2P_2$: C, 73.95; H, 4.57; N, 2.78. Found: C, 73.63; H, 4.28; N, 2.75. FT IR (KBr disc) cm^{-1}: υ_{CO}: 1656 vs, $\upsilon_{C=C}$: 1433 m. ^1H NMR (400 MHz, $CDCl_3$): δ 7.84 (s, 3H, Ar), 7.48-7.43 (m, 8H, Ar), 7.34–7.33 (m, 12H, Ar). $^{31}P\{^1H\}$ NMR (162 MHz, $CDCl_3$): δ 17.5 (s).

Synthesis of [$Ru_2Cl_4(NCCH_3)$(*p*-cymene){2,6-{$Ph_2PC(O)$}$_2$(C_5H_3N)}] (2)

A solution of **1** (0.050 g, 0.099 mmol) in CH_2Cl_2 (5 mL) was added dropwise to a solution of [Ru(η^6-*p*-cymene)Cl_2]$_2$ (0.060 g, 0.099 mmol) in CH_3CN (3 mL) during which time the color of the solution turned from orange to deep blue. The reaction was allowed to stir for 4 h. The solution was dried under reduced pressure and the residue redissolved in CH_2Cl_2 (5 mL) followed by saturation with 2 mL of petroleum ether to obtain crystals of **2**. 71.2% (0.072 g). Mp: 221–223 °C. Anal. Calcd. for $C_{43}H_{40}Cl_4N_2O_2P_2Ru_2 \cdot CH_2Cl_2$: C, 47.71; H, 3.82; N, 2.53. Found: C, 48.15; H, 3.62; N, 2.61. FT IR (KBr disc) cm^{-1}: υ_{CO}: 1677 s, 1648 s, $\upsilon_{C=C}$: 1382 m. ^1H

Dalton Transactions Accepted Manuscript

NMR (400 MHz, $CDCl_3$): δ 8.51 (d, 1H, Ar, $^3J_{HH}$ = 8.0 Hz), 8.32 (t, 4H, Ar, $^3J_{HH}$ = 8.0 Hz), 7.83-7.78 (m, 5H, Ar), 7.75(d, 1H, Ar, $^3J_{HH}$ = 7.6 Hz), 7.44-7.35 (m, 12H, Ar), 5.63 (d, 2H, Cym, $^3J_{HH}$ = 5.5 Hz), 5.47 (d, 2H, Cym, $^3J_{HH}$ = 5.5 Hz), 5.23 (s, 2H, CH_2Cl_2), 2.67 (s, 3H, CH_3CN), 2.61 (m, 2H, CH), 1.67 (s, 6H, CH_3), 0.97 (d, 12H, CH_3, $^3J_{HH}$ = 7.0 Hz). $^{31}P\{^1H\}$ NMR (162 MHz, $CDCl_3$): δ 79.5 (d, 1P, $^4J_{PP}$ = 6.5 Hz), 28.3 (d, 1P, $^4J_{PP}$ = 6.5 Hz).

Synthesis of [RuCl(NCCH$_3$)$_2${2,6-{Ph$_2$PC(O)}$_2$(C$_5$H$_3$N)}](ClO$_4$) (3)

A mixture of [Ru(η^6-*p*-cymene)Cl_2]$_2$ (0.030 g, 0.049 mmol) and $AgClO_4$ (0.020 g, 0.099 mmol) was stirred for 1 h in 6 mL of CH_3CN. The reaction mixture was filtered and added to a solution of **1** (0.050 g, 0.099 mmol) in CH_3CN (8 mL) during which time the color of the solution turned to deep brown. The reaction was allowed to stir for 3 h. The solution was dried under reduced pressure and the residue redissolved in CH_2Cl_2 (4 mL) followed by saturation with 2 mL of petroleum ether to obtain analytically pure **3** as brown solid. 94.2% (0.077 g). Mp: 268-270 °C. Anal. Calcd. for $C_{35}H_{29}Cl_2N_3O_6P_2Ru$: C, 51.17; H, 3.56; N, 5.11. Found: C, 51.58; H, 3.74; N, 5.38. FT IR (KBr disc) cm^{-1}: υ_{MeCN}: 2346 m, υ_{CO}: 1681 s, $\upsilon_{C=C}$: 1434 m, υ_{C-H}: 1094 s. ^1H NMR (400 MHz, $CDCl_3$): δ 8.11 (s, 3H, Ar), 7.84-7.77 (m, 8H, Ar), 7.63–7.41 (m, 12H, Ar), 2.60(s, 3H, CH_3CN), 1.80(s, 3H, CH_3CN). $^{31}P\{^1H\}$ NMR (162 MHz, $CDCl_3$): δ 51.9 (s).

Synthesis of [Ru(η^5-C$_5$H$_5$){2,6-{Ph$_2$PC(O)}$_2$(C$_5$H$_3$N)}](OTf) (4)

A mixture of [Ru(η^5-C_5H_5)Cl(PPh_3)$_2$] (0.029 g, 0.04 mmol) and AgOTf (0.0103 g, 0.04 mmol) was stirred for 4 h in 10 mL of CH_3CN. The reaction mixture was filtered trhough celite and added to a solution of **1** (0.020 g, 0.04 mmol) in CH_3CN (10 mL) during which time the color of the solution turned to dark yellow. The reaction was allowed to stir for 6 h. The solution was

Dalton Transactions Accepted Manuscript

dried under reduced pressure and the residue redissolved in CH_2Cl_2 (2 mL) followed by saturation with 2 mL of petroleum ether to obtain analytically pure **4** as dark yellow solid. 61% (0.019 g). Mp: 128-130 °C. Anal. Calcd. for $C_{37}H_{28}F_3NO_5P_2RuS$: C, 54.28 ; H, 3.44; N, 1.71. Found: C, 54.43; H, 3.19; N, 1.78. LRMS Calc for $C_{37}H_{28}F_3N_3O_5P_2RuS$ (M-OTf+Na): 693.0536, Found: 693.1315. ^{1}H NMR (500 MHz, $CDCl_3$): δ 7.37-7.06 (m, H, Ar), 4.49 (s, 5H, Cp), 2.25 (s, 3H, CH_3CN). ^{19}F{^{1}H} NMR (470 MHz, $CDCl_3$): δ -78.0 (s). ^{31}P{^{1}H} NMR (202 MHz, $CDCl_3$): δ 42.37 (s).

Synthesis of [RhCl{2,6-{$Ph_2PC(O)$}$_2$(C_5H_3N)}] (5)

The ligand **1** (0.035 g, 0.069 mmol) and $[Rh(COD)Cl]_2$ (0.017 g, 0.035 mmol) were placed in a round bottom flask and CH_2Cl_2 (6 mL) was added. The resulting solution was allowed to stir for 4 h, upon which the solution turned deep brown in color. The solution was concentrated to small bulk (4 mL) and saturated with 2 mL of petroleum ether to get analytically pure **5** as brown solid. Yield: 79% (0.035 g). Mp: 235-237 °C (dec). Anal. Calcd. for $C_{31}H_{23}ClNO_2P_2Rh$: C, 58.01; H, 3.61; N, 2.18. Found: C, 58.20; H, 3.60; N, 2.56. FT IR (KBr disc) cm^{-1}: υ_{CO}: 1692 vs, $\upsilon_{C=C}$: 1436 m. ^{1}H NMR (400 MHz, $CDCl_3$): δ 8.27 (m, 2H, Ar), 7.98 (m, 1H, Ar), 7.89–7.84 (m, 8H, Ar), 7.69-7.47 (m, 4H, Ar), 7.44-7.28 (m, 8H, Ar). ^{31}P{^{1}H} NMR (162 MHz, $CDCl_3$): δ 37.6 (d, $^1J_{RhP}$ = 104.3 Hz).

Synthesis of [NiCl{2,6-{$Ph_2PC(O)$}$_2$(C_5H_3N)}](BF_4) (6)

A solution of $[Ni(DME)Cl_2]$ (0.0088 g, 0.04 mmol) in 4 mL of dichloromethane was added dropwise to a solution of $AgClO_4$ (0.0078 g, 0.04 mmol) in acetonitrile (4 mL) and the reaction mixture was allowed to stir for 4 h to give a colorless solution. The solution was filtered through

Dalton Transactions Accepted Manuscript

a frit and the filtrate was added to the solution of **1** (0.02 g, 0.04 mmol) in CH_2Cl_2 (6 mL) and the reaction mixture was allowed to stir for 4 h. The solvent was removed under vaccum to obtain analytically pure product of **6** as dark brown solid. Yield: 90% (0.025 g). Mp: 155-160 °C. Anal. Calcd. for $C_{31}H_{23}ClNO_2P_2NiBF_4$: C, 54.40; H, 3.39; N, 2.05. Found: C, 54.13; H, 3.21; N, 1.73. HRMS Calc for $C_{31}H_{23}ClNNiO_2P_2$ (M-Cl+Na): 584.0450, Found: 584.0447. FT IR (KBr disc) cm^{-1}: υ_{CO}: 1685 m, $\upsilon_{C=C}$: 1418 m, υ_{C-H}: 1083 m. ^1H NMR (400 MHz, $CDCl_3$): δ 8.36 (t, 1H, Ar $^3J_{HH}$ = 7.6 Hz), 8.21 (d, 2H, Ar $^3J_{HH}$ = 7.6 Hz), 8.05 (br, s 8H, Ar), 7.66-7.63 (m, 4H, Ar), 7.57-7.54 (m, 8H, Ar). $^{31}P\{^1H\}$ NMR (162 MHz, $CDCl_3$): δ 28.5 (s).

Synthesis of [PdCl{2,6-{$Ph_2PC(O)$}$_2$(C_5H_3N)}](ClO_4) (7)

A solution of **1** (0.056 g, 0.112 mmol) in 5 mL of dichloromethane was added dropwise to a solution of $AgClO_4$ (0.023 g, 0.112 mmol) also in dichloromethane (5 mL) and the reaction mixture was allowed to stir for 1 h to give a yellow solution. [Pd(COD)Cl_2] (0.032 g, 0.112 mmol) in CH_2Cl_2 (5 mL) was added dropwise and the reaction mixture was allowed to stir for 2 h. The solution was filtered through a frit, concentrated to 4 mL and saturated with 2 mL of petroleum ether to get yellow crystals of **7**. Yield: 73% (0.060 g). Mp: 210-212 °C (dec). Anal. Calcd. for $C_{31}H_{23}Cl_2NO_6P_2Pd$: C, 49.99; H, 3.11; N, 1.88. Found: C, 49.65; H, 3.51; N, 2.23. FT IR (KBr disc) cm^{-1}: υ_{CO}: 1695 m, $\upsilon_{C=C}$: 1436 m, υ_{C-H}: 1092 m. ^1H NMR (400 MHz, $CDCl_3$): δ 8.43 (br s, 1H, Ar), 8.37 (br s, 2H, Ar), 8.02–7.98 (m, 8H, Ar), 7.64-7.61 (m, 4H, Ar), 7.56-7.53 (m, 8H, Ar). $^{31}P\{^1H\}$ NMR (162 MHz, $CDCl_3$): δ 45.2 (s).

Synthesis of [PtCl{2,6-{$Ph_2PC(O)$}$_2$(C_5H_3N) }](ClO_4) (8)

Dalton Transactions Accepted Manuscript

Compound **8** was synthesized by a procedure similar to that of **7** by using **1** (0.042 g, 0.084 mmol), $AgClO_4$ (0.017 g, 0.084 mmol) and [Pt(COD)Cl_2] (0.031 g, 0.084 mmol). Yield: 69% (0.048 g). Mp: 170-173 °C (dec). Anal. Calcd. for $C_{31}H_{23}Cl_2NO_6P_2Pt$: C, 44.67; H, 2.78; N, 1.68. Found: C, 44.95; H, 2.61; N, 1.96. FT IR (KBr disc) cm^{-1}: υ_{CO}: 1678 vs, $\upsilon_{C=C}$: 1434 m, υ_{C-H}: 1097 m. ^1H NMR (300 MHz, $CDCl_3$): δ 8.17 (br s, 1H, Ar), 8.09 (br s, 2H, Ar), 7.96–7.89 (m, 8H, Ar), 7.69-7.63 (m, 4H, Ar), 7.51-7.48 (m, 8H, Ar). $^{31}P\{^1H\}$ NMR (121 MHz, $CDCl_3$): δ 32.9 (s, $^1J_{PtP}$ = 2733 Hz).

Synthesis of [CuCl{2,6-{$Ph_2PC(O)$}$_2$(C_5H_3N)}] (9)

A solution of **1** (0.08 g, 0.159 mmol) in dichloromethane (8 mL) was added dropwise to a solution of CuCl (0.016 g, 0.159 mmol) in CH_3CN (4 mL). The reaction mixture was stirred for 3 h to give a dark brown solution. The solution was concentrated to 6 mL and stored at -20 ^oC to obtain **9** as dark brown solid. Yield: 87.2% (0.069 g). Mp: 208-210 °C (dec). Anal. Calcd. for $C_{31}H_{23}ClNO_2P_2Cu\cdot 0.5\ CH_2Cl_2$: C, 58.66; H, 3.75; N, 2.17. Found: C, 58.79; H, 3.92; N, 2.25. FT IR (KBr disc) cm^{-1}: υ_{CO}: 1677 vs, $\upsilon_{C=C}$: 1433 m, υ_{C-H}: 1258 s, 1093 vs, 1023 vs. ^1H NMR (400 MHz, $CDCl_3$): δ 8.09 (br s, 3H, Ar), 7.49 (br s, 8H, Ar), 7.33–7.31 (m, 4H, Ar), 7.23-7.20 (m, 8H, Ar), 5.23 (s, CH_2Cl_2). $^{31}P\{^1H\}$ NMR (162 MHz, $CDCl_3$): δ -0.08 (s). MS (EI): *m*/*z* 566.1, (M^+-Cl).

Synthesis of [CuBr{2,6-{$Ph_2PC(O)$}$_2$(C_5H_3N)}] (10)

Compound **10** was synthesized by a procedure similar to that of **9** using CuBr (0.014 g, 0.099 mmol) and **1** (0.050 g, 0.099 mmol). Yield: 85% (0.084 g). Mp: 191-192 °C (dec). Anal. Calcd. for $C_{31}H_{23}BrNO_2P_2Cu\cdot CH_2Cl_2$: C, 52.52; H, 3.44; N, 1.91. Found: C, 52.98; H, 3.10; N, 2.37. FT

Dalton Transactions Accepted Manuscript

IR (KBr disc) cm^{-1}: υ_{CO}: 1680 s, $\upsilon_{C=C}$: 1430 m, υ_{C-H}: 1258 vs, 1093 vs, 1023 vs. ^{1}H NMR (400 MHz, $CDCl_3$): δ 8.09 (br s, 3H, Ar), 7.50 (br s, 8H, Ar), 7.34 (t, 4H, Ar, $^3J_{HH}$ = 7.3 Hz), 7.23-7.22 (m, 8H, Ar), 5.22 (s, CH_2Cl_2). ^{31}P{^{1}H} NMR (162 MHz, $CDCl_3$): δ -0.18 (s). MS (EI): *m*/*z* 566.0, (M^+-Cl).

Synthesis of [CuI{2,6-{$Ph_2PC(O)$}$_2$(C_5H_3N)}] (11)

Compound **11** was synthesized by a procedure similar to that of **9** using CuI (0.015 g, 0.079 mmol) and **1** (0.040 g, 0.079 mmol). Yield: 91% (0.072 g). Mp: 238-239 °C (dec). Anal. Calcd. for $C_{31}H_{23}INO_2P_2Cu$: C, 53.65; H, 3.34; N, 2.01. Found: C, 53.90; H, 2.97; N, 2.36. FT IR (KBr disc) cm^{-1}: υ_{CO}: 1683 vs, $\upsilon_{C=C}$: 1436 m, υ_{C-H}: 1258 m, 1093 vs, 1020 m. ^{1}H NMR (400 MHz, $CDCl_3$): δ 7.55 (br s, 3H, Ar), 7.54 (br s, 8H, Ar), 7.40–7.38 (m, 4H, Ar), 7.29-7.27 (m, 8H, Ar). ^{31}P{^{1}H} NMR (162 MHz, $CDCl_3$): δ -0.8 (s). MS (EI): *m*/*z* 566.1, (M^+-Cl).

Synthesis of [Cu($NCCH_3$){2,6-{$Ph_2PC(O)$}$_2$(C_5H_3N)}](BF_4) (12)

A solution of **1** (0.05 g, 0.099 mmol) in acetonitrile (10 mL) was added dropwise to a solution of [Cu($NCCH_3$)$_4$](BF_4) (0.0312 g, 0.099mmol) in CH_3CN (5 mL). The reaction mixture was stirred for 4 h to give a dark brown solution. The solvent was evaporated by vaccum to obtain **12** as dark brown solid. Yield: 80% (0.054 g). Mp: 170-173 °C. Anal. Calcd. for $C_{33}H_{26}N_2O_2P_2CuBF_4$: C, 57.05; H, 3.77; N, 4.03. Found: C, 56.61; H, 3.58; N, 4.15. HRMS Calc for $C_{33}H_{26}N_2O_2P_2Cu$ (M-$NCCH_3$): 584.0450, Found: 584.0447. FT IR (KBr disc) cm^{-1}: υ_{MeCN}:2281 υ_{CO}: 1683 vs, $\upsilon_{C=C}$: 1436 m, υ_{C-H}: 1261 s, 1061 vs. ^{1}H NMR (400 MHz, $CDCl_3$): δ 8.40 (t, 1H, Ar $^3J_{HH}$ = 7.26 Hz), δ 8.33 (d, 2H, Ar $^3J_{HH}$ = 7.3 Hz) 7.49-7.46 (br s, 12H, Ar), 7.38–

Dalton Transactions Accepted Manuscript

7.34 (m, 8H, Ar), 5.29 (s, CH_2Cl_2), 2.22 (s, 3H, CH_3CN). $^{31}P\{^1H\}$ NMR (162 MHz, $CDCl_3$): δ 0.6 (s).

Synthesis of [Cu{2,6-{$Ph_2PC(O)$}$_2$(C_5H_3N)}$_2$](BF_4) (13)

A solution of **1** (0.05 g, 0.099 mmol) in acetonitrile (10 mL) was added dropwise to a solution of [Cu($NCCH_3$)$_4$](BF_4) (0.0155 g, 0.05mmol) in CH_3CN (5 mL). The reaction mixture was stirred for 3 h to give a dark brown solution. The solvent was evaporated by vaccum to obtain **13** as dark brown solid. Yield: 93% (0.053 g). Mp: 160-165 °C. Anal. Calcd. for $C_{62}H_{46}CuN_2O_4P_4BF_4$: C, 64.35; H, 4.01; N, 2.42. Found: C, 64.53; H, 3.76; N, 1.98. FT IR (KBr disc) cm^{-1}: υ_{CO}: 1682 vs, 1649 vs, $\upsilon_{C=C}$: 1481 m, 1434 m, υ_{C-H}: 1056 vs. ^1H NMR (500 MHz, $CDCl_3$): δ 8.19 (br, s 2H, Ar), 7.96 (d, 4H, Ar $^3J_{HH}$ = 7.1 Hz), 7.32–7.29 (m, 8H, Ar), 7.07-7.06 (m, 32H, Ar), 2.003 (s, 3H, CH_3CN). $^{31}P\{^1H\}$ NMR (202 MHz, $CDCl_3$): δ 6.0 (br, s).

Synthesis of [$AgClO_4${2,6-{$Ph_2PC(O)$}$_2$(C_5H_3N)}] (14)

A solution of **1** (0.040 g, 0.079 mmol) in 5 mL of THF was added dropwise to a solution of $AgClO_4$ (0.016 g, 0.079 mmol) in THF (4 mL) and the reaction mixture was allowed to stir for 1 h to give a yellow solution. The solution was dried under reduced pressure and the residue redissolved in CH_2Cl_2 (4 mL) followed by saturation with 1 mL of petroleum ether to give **14** as yellow solid. Yield: 83% (0.066 g). Mp: 130-132 °C (dec). Anal. Calcd. for $C_{31}H_{23}ClNO_6P_2Ag$: C, 52.38; H, 3.26; N, 1.97. Found: C, 52.44; H, 3.63; N, 2.31. FT IR (KBr disc) cm^{-1}: υ_{CO}: 1680 m, $\upsilon_{C=C}$: 1436 m, υ_{C-H}: 1258 s, 1093 vs. ^1H NMR (400 MHz, $CDCl_3$): δ 8.23 (d, 2H, Ar, $^3J_{HH}$ = 8.5 Hz), 8.16 (m, 1H, Ar), 7.56–7.51 (m, 8H, Ar), 7.48-7.45 (m, 4H, Ar), 7.37-7.34 (m, 8H, Ar). $^{31}P\{^1H\}$ NMR (162 MHz, $CDCl_3$): δ 4.92 (br, s). MS (EI): *m/z* 708.9 (M^+).

Dalton Transactions Accepted Manuscript

Synthesis of [AgBr{2,6-{$Ph_2PC(O)$}$_2$(C_5H_3N)}] (15)

Compound **15** was synthesized by a procedure similar to that of **14** using AgBr (0.019 g, 0.099 mmol) and **1** (0.050 g, 0.099 mmol). Yield: 85% (0.085 g). Mp: 220-221 °C (dec). Anal. Calcd. for $C_{31}H_{23}BrNO_2P_2Ag$: C, 53.86; H, 3.35; N, 2.02. Found: C, 53.63; H, 3.73; N, 2.37. FT IR (KBr disc) cm^{-1}: υ_{CO}: 1674 vs, $\upsilon_{C=C}$: 1433 m, υ_{C-H}: 1261 m. ^1H NMR (400 MHz, $CDCl_3$): δ 8.17 (br s, 3H, Ar), 7.50-7.48 (m, 8H, Ar), 7.38–7.34 (m, 4H, Ar), 7.26-7.22 (m, 8H, Ar). $^{31}P\{^1H\}$ NMR (162 MHz, $CDCl_3$): δ 5.56 (br, s). MS (EI): *m*/*z* 610.1, (M^+-Br)

Synthesis of [AuCl{2,6-{$Ph_2PC(O)$}$_2$(C_5H_3N)}](16)

A solution of **1** (0.040 g, 0.079 mmol) in 5 mL of CH_2Cl_2 was added dropwise to a solution of AuCl(SMe_2) (0.023 g, 0.079 mmol) also in CH_2Cl_2 (3 mL) and the reaction mixture was stirred for 2 h to give a bright orange solution. The solution was concentrated to small bulk (3 mL) and saturated with 1 mL of petroleum ether to get analytically pure **16** as a bright orange solid. Yield: 88.2% (0.070 g). Mp: 165-167 °C (dec). Anal. Calcd. for $C_{31}H_{23}ClNO_2P_2Au$: C, 50.59; H, 3.15; N, 1.90. Found: C, 50.87; H, 2.95; N, 2.14. FT IR (KBr disc) cm^{-1}: υ_{CO}: 1680 vs, $\upsilon_{C=C}$: 1435 m, 1384 s, υ_{C-H}: 1094 m. ^1H NMR (400 MHz, $CDCl_3$): δ 8.02 (br s, 3H, Ar), 7.44–7.38 (m, 12H, Ar), 7.33-7.29 (m, 8H, Ar). $^{31}P\{^1H\}$ NMR (162 MHz, $CDCl_3$): δ 24.6 (s). MS (EI): *m*/*z* 700.1, (M^+-Cl).

Synthesis of [Au_2Cl_2{2,6-{$Ph_2PC(O)$}$_2$(C_5H_3N)}] (17)

To a CH_2Cl_2 (3 mL) solution of **1** (0.030 g, 0.059 mmol) was added dropwise a solution of AuCl(SMe_2) (0.035 g, 0.119 mmol) also in CH_2Cl_2 (4 mL) and reaction mixture was stirred for 2 h to give a yellow solution. The solution was concentrated to 5 mL and saturated with 1 mL of

Dalton Transactions Accepted Manuscript

petroleum ether to get yellow crystals of **17**. Yield: 86.4% (0.051 g). Mp: 178-180 °C (dec). Anal. Calcd. for $C_{31}H_{23}Cl_2NO_2P_2Au_2$: C, 38.45; H, 2.39; N, 1.45. Found: C, 38.20; H, 2.12; N, 1.66. FT IR (KBr disc) cm^{-1}: υ_{CO}: 1678 vs, $\upsilon_{C=C}$: 1434 m, υ_{C-H}: 1097 m. ^1H NMR (400 MHz, $CDCl_3$): δ 7.99 (s, 3H, Ar), 7.46–7.38 (m, 12H, Ar), 7.35-7.31 (m, 8H, Ar). $^{31}P\{^1H\}$ NMR (162 MHz, $CDCl_3$): δ 38.5 (s).

Computational Methods

All geometries were optimized using the Gaussian 09[30] suite of quantum chemical programs. All the geometries were optimized at the B3LYP[31], M06[32] functional and characterized as true minima on the potential energy surfaces by evaluating the Hessian indices (Number of imaginary frequencies = 0). The 6-31G** basis set was used for all atoms except for the metal ion and iodine. The effective core potential basis set (SDD) is employed for metals (Rh, Ru and Au).[33] Molecular orbital analysis has been done to find the HOMO-LUMO energy gap using the iop(6/7=3) at B3LYP/6-31G**, SDD level of theory. Molecular orbital compositions of metal and ligands were analyzed using AOMix−CDA program[17] using the wave functions generated at the B3LYP/6-31G**, SDD level of theory and using Gaussian 03 suite of quantum chemical programs.[34] Bader developed theory of atoms in molecules (AIM) which is applied to characterize weak interactions.[35] Atoms in molecules (AIM) analysis calculations were carried out using AIM2000 software.[36]

X-Ray Crystallography

Crystal of each of the compounds **1**, **2**, **5**, and **17** suitable for X-ray crystal analysis were mounted on a Cryoloop with a drop of Paratone oil and placed in the cold nitrogen stream of the

Dalton Transactions Accepted Manuscript

Kryoflex attachment of the Bruker APEX CCD diffractometer. A full sphere of data was collected using combination of three sets of 400 scans in ω (0.5º per scan) at φ = 0, 90, and 180º plus two sets of 800 scans in φ (0.45º per scan) at ω = -30 and 210º using the SMART[37] software package, or the APEX2[38] program suite. The raw data were reduced to F^2 values using the SAINT software[39] and a global refinements of unit cell parameters using *ca*. 4575-9954 reflections chosen from the full data set were performed. Multiple measurements of equivalent reflections provided the basis for an empirical absorption correction as well as a correction for any crystal deterioration during the data collection (SADABS[40]). The structures were solved by Patterson or direct methods and refined by full-matrix least-squares procedures using the SHELXTL program package.[41] The details of X-ray structural determinations are given in Table 3. Crystallographic data for the structures reported in this paper have been deposited with the Cambridge Crystallographic Data Centre as supplementary publication no. CCDC 1038055 (compound **1**), 1038057 (compound **2**), 1038058 (compound **5**), and 1038056 (compound **17**).

Associated content

Supporting Information

X-ray crystallographic files in CIF format for the structure determinations of and **1**, **2**, **5** and **17**, and computational details. This material is available free of charge via the Internet at http://pubs.rsc.org.

Author information

Corresponding Authors

*E-mail: krishna@chem.iitb.ac.in or msb_krishna@iitb.ac.in (M. S. Balakrishna), sunoj@chem.iitb.ac.in (R. B. Sunoj). Fax: +91-22-2572-3480/2576-7152.

Acknowledgements

Dalton Transactions Accepted Manuscript

We are grateful to the Science & Engineering Research Board, New Delhi, for financial support of this work through grant *No.SB/S1/IC-08/2014*. P.K. thanks CSIR, New Delhi for Research Fellowship (JRF & SRF). We also thank the Department of Chemistry Instrumentation Facilities, IIT Bombay, for spectral and analytical data and J.T.M. thanks the Louisiana Board of Regents for the purchase of the CCD diffractometer and the Chemistry Department of Tulane University for support of the X-ray laboratory.

References

1. (a) J. T. Singleton, *Tetrahedron* 2003, **59**, 1837-1857; (b) G. van Koten, *J. Organomet. Chem.*, 2013, **730**, 156-164; (c) M. E. van der Boom and D. Milstein, *Chem. Rev.*, 2003, **103**, 1759-1792; (d) N. Selander, and K. J. Szabo, *Chem. Rev.*, 2011, **111**, 2048-2076; (e) M. Albrecht and G. van Koten, *Angew. Chem. Int. Ed.*, 2001, **40**, 3750-3781; (f) G. van Koten, D. Milstein, J. Hawk and S. Craig, *Organometallic Pincer Chemistry*; Springer Berlin, 2013; **40**, 319-352; (g) W. C. Yount, D. M. Loveless, and S. L. Craig, *Angew. Chem. Int. Ed.*, 2005, **44**, 2746-2748; (h) J. I. van der Vlugt and J. N. H. Reek, *Angew. Chem. Int. Ed*., 2009, **48**, 8832-8846.
2. (a) J. M. Longmire, X. Zhang and M. Shang, *Organometallics*, 1998, **17**, 4374-4379; (b) J. Aydin, K. S. Kumar, M. J. Sayah, O. A. Wallner and K. J. Szabo, *J. Org. Chem.*, 2007, **72**, 4689-4697; (c) F. Gorla, A. Togni, L. M. Venanzi, A. Albinati and F. Lianza, *Organometallics*, 1994, **13**, 1607-1616.
3. (a) A. Alzamly, S. Gambarotta and I. Korobkov, *Organometallics*, 2013, **32**, 7204-7212; (b) C. Klemps, E. Payet, L. Magna, L. Saussine, X. F. Le Goff and P. Le Floch, *Chem. Eur. J.*, 2009, **15**, 8259-8268.
4. (a) M. C. Haibach, S. Kundu, M. Brookhart and A. S. Goldman, *Acc. Chem. Res.*, 2012, **45**, 947-958; (b) P.-Y. Shi, Y.-H. Liu, S.-M. Peng and S.-T. Liu, *Organometallics*, 2002, **21**, 3203-3207.
5. (a) A. Choualeb, A. J. Lough and D. G. Goussev, *Organometallics*, 2007, **26**, 3509-3515; (b) A. Friedrich, R. Ghosh, R. Kolb, E. Herdtweck and S. Schneider, *Organometallics*, 2009, **28**, 708-718; (c) D. Benito-Garagorri, L. G. Alves, M. Puchberger, K. Mereiter, L. F. Veiros, M. J. Calhorda, M. D. Carvalho, L. P. Ferreira, M. Godinho and K. Kirchner,

Dalton Transactions Accepted Manuscript

Organometallics, 2009, **28**, 6902-6914; (d) S. S. Rozenel, J. B. Kerr and J. Arnold, *Dalton Trans.*, 2011, 10397-10405; (e) S. S. Rozenel, R. Padilla and J.Arnold, *Inorg. Chem.*, 2013, **52**, 11544-11550; (f) D. A. Smith, D. E. Herbert, J. R. Walensky and O. V. Ozerov, *Organometallics*, 2013, **32**, 2050-2058.

6. (a) K. Arashiba, S. Kuriyama, K. Nakajima and Y. Nishibayashi, *Chem. Commun.*, 2013, **49**, 11215-11217; (b) Y. Nakajima, Y. Okamoto, Y.-H. Chang, and F. Ozawa *Organometallics*, 2013, **32**, 2918-2925; (c) I. Gottker-Schnetmann, P. White and M. Brookhart, *J. Am. Chem. Soc.*, 2004, **126**, 1804-1811; (d) D. Morales-Morales, R. Redan, C. Yung and C. M. Jensen, *Inorg. Chim.*, *Acta*, 2004, **357**, 2953-2956; (e) D. Benito-Garagorri, E. Becker, J. Wiedermann, W. Lackner, M. Pollak, K. Mereiter, J. Kisala and K. Kirchner, *Organometallics*, 2006, **25**, 1900-1913; (f) D. Benito-Garagorri, J. Wiedermann, M. Pollak, K. Mereiter and K. Kirchner, *Organometallics*, 2007, **26**, 217-222.

7. (a) J. Meiners, A. Friedrich, E. Herdtweck and S. Schneider, *Organometallics*, 2009, **28**, 6331-6338; (b) L. Schwartsburd, M. A. Iron, L. Konstantinovski, E. Ben-Ari and D. Milstein, *Organometallics*, 2011, **30**, 2721-2729; (c) S. W. Kohl, L. Weiner, L. Schwartsburd, L. Konstantinovski, L. J. W. Shimon, Y. Ben-David, M. A. Iron and D. Milstein, *Science*, 2009, **324**, 74-77; (d) Y.-H. Chang, Y. Nakajima, H. Tanaka, K. Yoshizawa and F. Ozawa, *J. Am. Chem. Soc.*, 2013, **135**, 11791-11794; (e) M. Feller, M. A. Iron, L. J. W. Shimon, Y. Diskin-Posner, G. Leitus and D. Milstein, *J. Am. Chem. Soc.*, 2008, **130**, 14374-14375; (f) J. I. van der Vlugt, E. A. Pidko, R. C. Bauer, Y. Gloaguen, M. K. Rong and M. Lutz, *Chem. Eur. J.,* 2011, **17**, 3850-3854.

8. (a) K. Arashiba, Y. Miyake and Y.Nishibayashi, *Nat. Chem*., 2011, **3**, 120-125; (b) B. Bichler, C. Holzhacker, B. Stöger, M. Puchberger, L. F. Veiros and K. Kirchner, *Organometallics*, 2013, **32**, 4114-4121; (c) M. Vogt, O. Rivada-Wheelaghan, M. A. Iron, G. Leitus, Y. Diskin-Posner, L. J. W. Shimon, Y. Ben-David and D. Milstein, *Organometallics*, 2013, **32**, 300-308.

9. (a) J. Zhang, G. Leitus, Y. Ben-David and D. Milstein, *J. Am. Chem. Soc.*, 2005, **127**, 10840-10841; (b) C. Gunanathan, Y. Ben-David and D. Milstein, *Science*, 2007, **317**, 790-792; (c) X. Yang, *ACS Catal.*, 2013, **3**, 2684-2688; (d) E. Balaraman, E. Fogler and D. Milstein, *Chem. Commun.*, 2012, **48**, 1111-1113; (e) G. A. Filonenko, M. P. Conley,

Dalton Transactions Accepted Manuscript

C. Copéret, M. Lutz, E. J. M. Hensen and E. A. Pidko, *ACS Catalysis*, 2013, **3**, 2522-2526.

10. (a) M. Bertoli, A. Choualeb, D. G. Gusev, A. J. Lough, Q. Major and B. Moore, *Dalton Trans.*, 2011, **40**, 8941-8949; (b) E. Balaraman, B. Gnanaprakasam, L. J. W. Shimon and D. Milstein, *J. Am. Chem. Soc.*, 2010, **132**, 16756-16758; (c) H. Zeng and Z. Guan, *J. Am. Chem. Soc.*, 2011, **133**, 1159-1161.
11. (a) H. Albers, W. Kunzel and W. E. Scheeber, *Chem. Ber.*, 1952, **85**, 239-249; (b) R. G. Kostyanovsky, V. V. Yakshin and S. L. Zimont, *Tetrahedron*, 1968, **24**, 2995-3000; (c) H. Kunzek, M. Braun, E. Nesener and K. Rühlmann, *J. Organomet. Chem.*, 1973, **49**, 149-156; (d) K. Issleib, H. Schmidt and H. Meyer, *J. Organomet. Chem.*, 1978, **160**, 47-57; (e) A. Varshney and G. M. Gray, *Inorg. Chim. Acta*, 1988, **148**, 215-222; (f) R. Angharad Baber, M. L. Clarke, A. Guy Orpen and D. A. Ratcliffe, *J. Organomet. Chem.*, 2003, **667**, 112-119; (h) A. R. Barron, S. W. Hall and A. H. Cowley, *J. Chem. Soc., Chem. Commun.*, 1987, 1753.
12. P. Kumar, M. M. Siddiqui, Y. Reddi, J. T. Mague, R. B. Sunoj and M. S. Balakrishna, *Dalton Trans.*, 2013, **42**, 11385-11399.
13. (a) M. S. Balakrishna, R. Panda and J. T. Mague, *Inorg. Chem.*, 2001, **40**, 5620-5625; (b) S. Priya, M. S. Balakrishna, J. T. Mague and S. M. Mobin, *Inorg. Chem.*, 2003, **42**, 1272-1281; (c) C. Ganesamoorthy, M. S. Balakrishna and J. T. Mague, *Inorg. Chem.*, 2009, **48**, 3768-3782; (d) M. S. Balakrishna, P. Kumar, B. Punji and J. T. Mague, *J. Organomet. Chem.*, 2010, **695**, 981-986; (e) G. S. Ananthnag, S. Kuntavalli, J. T. Mague and M. S. Balakrishna, *Inorg. Chem.*, 2012, **51**, 5919-5930; (f) S. Rao, J. T. Mague and M. S. Balakrishna, *Dalton Trans.,* 2013, **42**, 11695-11708; (g) B. Chaubey, S. M. Mobin and M. S. Balakrishna, *Dalton Trans.*, 2014, **43**, 584-591.
14. The optimized geometry obtained at the M06/6-31G**, SDD level of theory is provided in Fig. S6 in the Supporting Information.
15. (a) H.-L. Kwong, W.-S. Lee, T.-S. Lai and W.-T. Wong, *Inorg. Chem. Commun.*, 1999, **2**, 66-69; (b) B. Crociani, S. Antonaroli, M. Burattini, P. Paoli and P. Rossi, *Dalton Trans.*, 2010, **39**, 3665-3672; (c) K. Sun, L. Wang and Z.-*X.* Wang, *Organometallics, 2*008, **27**, 5649-5656; (d) N. Liu, L. Wang and *Z.-X.* Wang, *Chem.* Commun., 2011, **47**, 1598-1600; (e) A. Scharf, I. Goldberg and A. Vigalok, *Inorg. Chem*. 2014, **53**, 12-14 (f)

Dalton Transactions Accepted Manuscript

D. L. J. Broere, L. L. Metz, B. De, Bruin, J. N. H. Reek, M. A. Siegler, and J. I. van der Vlugt, *Angew. Chem. Int. Ed*., doi:10.1002/anie.201410048.

16. (a) S. I. M. Paris, F. R. Lemke, R. Sommer, P. Lönnecke and E. Hey-Hawkins, *J. Organomet. Chem.*, 2005, **690**, 1807-1813; (b) T. J. Geldbach, A. B. Chaplin, K. D. Hänni, R. Scopelliti and P. J. Dyson, *Organometallics*, 2005, **24**, 4974-4980; (c) M. S. Balakrishna, D. Suresh, P. Kumar and J. T. Mague, *J. Organomet. Chem.*, 2011, **696**, 3616-3622; (d) E. E. Joslin, C. L. McMullin, T. B. Gunnoe, T. R. Cundari, M. Sabat and W. H. Myers, *Inorg. Chem.*, 2012, **51**, 4791-4801.
17. (a) S. I. Gorelsky, *AOMix: Program for Molecular Orbital Analysis*, York University, Toronto, Canada, http://www.sq-chem.net (b) S. I. Goreslsky and A. B. P. Lever, *J. Organomet. Chem.*, 2001, **635**, 187-196.
18. (a) D. Hermann, M. Gandelman, H. Rozenberg, L. J. W. Shimon and D. Milstein, *Organometallics*, 2002, **21**, 812-818; (b) W. Weng, C. Guo, R. Celenligil-Cetin, B. M. Foxman and O. V. Ozerov, *Chem. Commun.*, 2006, 197-199; (c) C. Gaviglio, Y. Ben-David, L. J. W. Shimon, F. Doctorovich and D. Milstein, *Organometallics*, 2009, **28**, 1917-1926; (d) S. K. Hanson, D. M. Heinekey, K. I. Goldberg, *Organometallics*, 2008, **27**, 1454-1463.
19. (a) J. I. van der Vlugt, E. A. Pidko, D. Vogt, M. Lutz, A. L. Spek and A. Meetsma, *Inorg. Chem.,* 2008, **47**, 4442-4444; (b) J. I. van der Vlugt, E. A. Pidko, D. Vogt, M. Lutz and A. L. Spek, *Inorg. Chem.*, 2009, **48**, 7513-7515.
20. (a) J. C. H. Kline and J. Turkevich, *J. Chem. Phys.*, 1944, **12**, 300-309; (b) S. Liu, R. Peloso and P. Braunstein, *Dalton Trans.*, 2010, **39**, 2563-2572.
21. Hahn, A. Vitagliano, F. Giordano and R. Taube, *Organometallics*, 1998, **17**, 2060-2066.
22. A. C. Tsipis, *Organometallics*, 2006, **25**, 2774-2781.
23. W. L. Armarego and D. D. Perrin, *Purification of Laboratory Chemicals, 4th ed, Butterworth-Heinemann Linacre House, Jordan Hill, Oxford, U. K.* 1996.
24. B. S. Furniss, A. J. Hannaford, P. W. G. Smith and A. R. Tatchell, *Vogel's Textbook of Practical Organic Chemistry, Fifth Edition, ELBS, England* 1989, 428–429.
25. G. J. Kubas, *Inorg. Synth*., 1979, **19**, 90-91.
26. M. C. Brandys, M. C. Jennings and R. J. Puddephatt, *J. Chem. Soc., Dalton Trans.,* 2000, 4601-4606.

Dalton Transactions Accepted Manuscript

27. M. A. Bennett, T. N. Huang, T. W. Matheson and A. K. Smith, *Inorg. Synth.*, 1982, **21**, 74-78.

28. G. Giordano and R. H. Crabtree, *Inorg. Synth.*, 1990, **28**, 88-90.

29. D. Drew and J. R. Doyle, *Inorg. Synth.*, 1990, **28**, 346-349.

30. M. J. Frisch, G. W. Trucks, H. B. Schlegel, G. E. Scuseria, M. A. Robb, J. R. Cheeseman, G. Scalmani, V. Barone, B. Mennucci, G. A. Petersson, H. Nakatsuji, M. Caricato, X. Li, H. P. Hratchian, A. F. Izmaylov, J. Bloino, G. Zheng, J. L. Sonnenberg, M. Hada, M. Ehara, K. Toyota, R. Fukuda, J. Hasegawa, M. Ishida, T. Nakajima, Y. Honda, O. Kitao, H. Nakai, T. Vreven, Jr, J. E. Peralta, F. Ogliaro, M. Bearpark, J. J. Heyd, E. Brothers, K. N. Kudin, V. N. Staroverov, R. Kobayashi, J. Normand, K. Raghavachari, A. Rendell, J. C. Burant, S. S. Iyengar, J. Tomasi, M. Cossi, N. Rega, J. M. Millam, M. Klene, J. E. Knox, J. B. Cross, V. Bakken, C. Adamo, J. Jaramillo, R. Gomperts, R. E. Stratmann, O. Yazyev, A. J. Austin, R. Cammi, C. Pomelli, J. W. Ochterski, R. L. Martin, K. Morokuma, V. G. Zakrzewski, G. A. Voth, P. Salvador, J. J. Dannenberg, S. Dapprich, A. D. Daniels, Farkas, J. B. Foresman, J. V. Ortiz, J. Cioslowski and D. J. Fox, *GAUSSIAN 09* (*Revision A.02*), Gaussian Inc. Wallingford CT, 2009.

31. (a) A. D. Becke, *Phys. Rev. A*, 1988, **38**, 3098-3100; (b) A. D. Becke, *J. Chem. Phys.*, 1993, **98**, 5648-5652; (c) C. Lee, W. Yang and R. G. Parr, *Phys. Rev. B*, 1988, **37**, 785-789.

32. (a) Y. Zhao and D. G. Truhlar, *Theor. Chem. Acc.*, 2008, **120**, 215-241. (b) Y. Zhao and D. G. Truhlar, *Acc. Chem. Res.*, 2008, **41**, 157-167.

33. (a) H. Stoll, P. Fuentealba, P. Schwerdtfeger, J. Flad, L. V. Szentpaly and H. Preuss, *J. Chem. Phys.*, 1984, **81**, 2732-2736; (b) M. Dolg, U. Wedig, H. Stoll and H. Preuss, *J. Chem. Phys.*, 1987, **86**, 866-872. (c) D. Andrae, U. Haussermann, M. Dolg, H. Stoll and H. Preuss, *Theor. Chim. Acta*, 1990, **77**, 123-141.

34. M. J. Frisch, G. W. Trucks, H. B. Schlegel, G. E. Scuseria, M. A. Robb, J. R. Cheeseman, J. A. Montgomery, Jr., T. Vreven, K. N. Kudin, J. C. Burant, J. M. Millam, S. S. Iyengar, J. Tomasi, V. Barone, B. Mennucci, M. Cossi, G. Scalmani, N. Rega, G. A. Petersson, H. Nakatsuji, M. Hada, M. Ehara, K. Toyota, R. Fukuda, J. Hasegawa, M. Ishida, T. Nakajima, Y. Honda, O. Kitao, H. Nakai, M. Klene, X. Li, J. E. Knox, H. P. Hratchian, J. B. Cross, V. Bakken, C. Adamo, J. Jaramillo, R. Gomperts, R. E. Stratmann, O. Yazyev, A. J. Austin, R. Cammi, C. Pomelli, J. W. Ochterski, P. Y. Ayala, K. Morokuma, G. A.

Dalton Transactions Accepted Manuscript

Voth, P. Salvador, J. J. Dannenberg, V. G. Zakrzewski, S. Dapprich, A. D. Daniels, M. C. Strain, O. Farkas, D. K. Malick, A. D. Rabuck, K. Raghavachari, J. B. Foresman, J. V. Ortiz, Q. Cui, A. G. Baboul, S. Clifford, J. Cioslowski, B. B. Stefanov, G. Liu, A. Liashenko, P. Piskorz, I. Komaromi, R. L. Martin, D. J. Fox, T. Keith, M. A. Al-Laham, C. Y. Peng, A. Nanayakkara, M. Challacombe, P. M. W. Gill, B. Johnson, W. Chen, M. W. Wong, C. Gonzalez, and J. A. Pople, *GAUSSIAN 03* (*Revision C.02*), Gaussian, Inc., Wallingford CT, 2004.

35. R. F. W. Bader, *Atoms in Molecules: A Quantum Theory*; Clarendon Press: Oxford, 1990.
36. (a) AIM2000 Version 2.0; Buro fur Innovative Software, SBK-Software: Bielefeld, Germany, 2002; (b) F. Biegler-Konig, J. Schonbohm and D. Bayles, *J. Comput. Chem*., 2001, **22**, 545-559. (c) F. Biegler-Konig, J. Schonbohm, *J. Comput. Chem*., 2002, **23**, 1489-1494.
37. Bruker-AXS *SMART, Version 5.625, Madison, WI,* 2000.
38. APEX2 *version 2.1-0, Bruker-AXS, Madison, WI,* 2006.
39. Bruker-AXS, *SAINT*, Madison, WI, 2006.
40. G. W. Sheldrick, *SADABS, versions 2.05 and 2007/2, University of Göttingen, Germany* 2002.
41. G. M. Sheldrick, SHELXS97 and SHELXL97; University of Göttingen; Germany 1997.

Dalton Transactions Accepted Manuscript

Table 1. Composition and energies of important Kohn–Sham orbitals of ruthenium pincer complex **2** obtained using the Wave Function Generated at the B3LYP/6-31G**, SDD level of theory

Orbital	Energy (in eV)	Orbital character
LUMO	-2.943	9.66% d_{xz} Ru(1), 90.34% (PNO and Ru(2))
HOMO	-5.274	90.17% d_{xz} Ru(1), 9.83% PNO
HOMO-29	-8.720	79.99% d_z^2 Ru(1), 20.01% (PNO and Ru(2))

Dalton Transactions Accepted Manuscript

Table 2 Selected bond distances (Å) and bond angles (°) for compounds **1**, **2**, **5** and **17**[a]

Parameter	2,6-{$Ph_2PC(O)$}$_2$(C_5H_3N) (**1**)			$Ru_2Cl_4(NCCH_3)$(*p*-cymene){2,6-{$Ph_2PC(O)$}$_2$(C_5H_3N)}] (**2**)			[RhCl{2,6-{$Ph_2PC(O)$}$_2$(C_5H_3N)}] (**5**)			[Au_2Cl_2 {2,6-{$Ph_2PC(O)$}$_2$(C_5H_3N)}] (**17**)		
		Exp.	Calculated		Exp.	Calculated		Exp.	Calculated		Exp.	Calculated
Bond distances (Å)	P1–C1	1.8195(16)	1.8435	Ru1–N1	1.981(3)	2.0053	Rh1– N1	2.0375(14)	2.0565	Au1–P1	2.2326(12)	2.3177
	P1–C7	1.8242(14)	1.8435	Ru1–N2	2.048(3)	2.0377	Rh1–P1	2.2523(6)	2.2866	Au2–P2	2.2270(11)	2.3190
	P1–C13	1.8585(16)	1.8986	Ru1–O2	2.146(2)	2.1781	Rh1– P2	2.2611(6)	2.2866	Au1–Cl2	2.3000(12)	2.3537
	P2–C20	1.8179(15)	1.8944	Ru1–P1	2.2260(8)	2.2392	Rh1–Cl1	2.3390(6)	2.3631	Au2–Cl1	2.2845(11)	2.3437
	P1–C26	1.8274(15)	1.8351	Ru1–Cl2	2.3883(8)	2.4230	P1–C13	1.8722(18)	1.8888	Au1–Au2	3.1445(7)	3.1573
	P1–C19	1.8698(16)	1.8945	Ru1–Cl1	2.3978(8)	2.4208	P2–C19	1.8720(17)	1.8888	P1–C13	1.881(4)	1.9044
	O1–C13	1.2114(17)	1.2131	Ru2–P2	2.3486(9)	2.3786	P1–C1	1.8257(17)	1.827	P2–C19	1.893(4)	1.9077
	O1–C19	1.2108(17)	1.2122	Ru2–Cl4	2.4039(8)	2.4389	P1–C7	1.8137(17)	1.8221	O1–C13	1.212(5)	1.2084
	N1–C14	1.3361(17)	1.3336	Ru2–Cl3	2.4193(9)	2.4329	P2–C20	1.8256(17)	1.8221	O2–C19	1.203(5)	1.2062
	N1–C18	1.3371(17)	1.3311	P1–C13	1.896(3)	1.9051	P2–C26	1.8192(18)	1.827			
				O1–C13	1.211(4)	1.2118	O1–C13	1.209(2)	1.2142			
				O2–C19	1.237(4)	1.2426	O2–C19	1.211(2)	1.2142			
				P2–C19	1.860(3)	1.8630						
Bond angles (°)	C1–P1–C7	104.97(7)	101.821	C14–N1–C18	118.1(3)	118.981	P1–Rh1–P2	153.105(17)	171.09	P1–Au1–Cl2	167.58(4)	169.714
	C1–P1–C13	100.11(7)	98.235	N1–Ru1–O2	77.69(9)	76.794	N1–Rh1–Cl1	176.71(4)	180.0	P2–Au2–Cl1	173.52(4)	170.714
	C7–P1–C13	100.60(6)	98.09	N1–Ru1–P1	86.79(7)	86.434	N1–Rh1–P1	84.39(4)	85.539	C13–P1–Au1	117.14(13)	112.40
	C20–P2–C26	102.81(7)	102.349	N1–Ru1–Cl1	85.46(7)	89.263	N1–Rh1–P2	85.10(4)	85.539	C19–P2–Au2	110.45(14)	125.188
	C20–P2–C19	102.83(7)	93.412	N1–Ru1–Cl2	91.87(7)	89.815	C13– P1–Rh1	99.98(6)	99.725	C20–P2–Au2	115.95(8)	113.581
	C26–P2–C19	100.73(6)	98.410	O2–Ru1–P1	164.38(6)	163.226	C19 –P2–Rh1	99.50(6)	99.723	C14–C13–P1	117.3(3)	115.895
	C14–N1–C18	117.03(12)	117.784	C13–P1–Ru1	99.25(10)	98.984	C14– C13– P1	112.07(12)	113.487	C18– C19–P2	117.3(3)	117.18
	C14– C13– P1	115.20(10)	115.419	C19–O2–Ru1	113.12(19)	113.138	C18 –C19 –P2	113.19(12)	113.488			
	C18– C19– P2	116.83(9)	114.615	C14–C13–P1	113.5(2)	113.072						
				C18–C19–P2	123.6(2)	125.156						
				P2–Ru2–Cl4	87.85(3)	87.254						
				P2–Ru2–Cl3	91.30(3)	86.889						
				C19–P2–Ru2	105.74(10)	103.776						

[a]The optimized geometrical parameters obtained at the M06/6-31G**, SDD level of theory

Dalton Transactions Accepted Manuscript

Table 3 Crystallographic Data for **1**, **2**, **5** and **17**

	1	**2**	**5**	**17**
formula	$C_{31}H_{23}NO_2P_2$	$C_{44}H_{42}Cl_6N_2O_3P_2Ru_2$	$C_{31}H_{23}ClNO_2P_2Rh$	$C_{31}H_{23}Au_2Cl_2NO_2P_2$
fw	503.44	1123.58	641.80	968.28
crystal system	Monoclinic	Triclinic	Monoclinic	Monoclinic
space group	P2(1)/n	P-1	P2(1)/c	P2(1)
a, Å	15.7730(15)	12.3052(14)	11.894(3)	8.4416(18)
b, Å	9.3471(9)	12.6279(14)	14.148(3)	17.820(4)
c, Å	18.1249(17)	15.3356(17)	15.675(4)	9.883(2)
α, deg	90.00	90.014(2)	90.00	90.00
β, deg	102.011(1)	93.922(2)	101.663(3)	91.510(3)
γ, deg	90.00	105.059(2)	90.00	90.00
V, $Å^3$	2613.7(4)	2295.4(4)	2583.4(10)	1486.2(5)
Z	4	2	4	2
ρ_{calc}, g cm^{-3}	1.279	1.626	1.650	2.164
μ (MoKα), mm^{-1}	0.195	1.119	0.920	10.178
F (000)	1048	1128	1296	908
Crystal size mm)	0.33×0.22×0.13	0.35×0.12×0.06	0.26×0.24×0.21	0.18×0.13×0.09
T, K	195(2)	100(2)	100(2)	100(2)
2θ range, deg	2.30-28.26	2.50-29.12	2.88-29.12	2.36-29.10
Total no. reflns	45044	40501	44962	25985
No. of indep. Reflns	6517	11568	6752	7441
R1[a]	0.0387	0.0408	0.0260	0.0202
wR_2[b]	0.1057	0.1096	0.0665	0.0438
GOF (F^2)	1.029	1.035	1.038	0.923

[a] $R = \Sigma||F_o|-|Fc||/\Sigma|F_o|$.

[b] $wR_2 = \{[\Sigma w(F_o^2-F_c^2)/\Sigma w(F_o^2)^2]\}^{1/2}$; $w = 1/[\sigma^2(F_o^2)+(xP)^2]$ where $P = (F_o^2+2F_c^2)/3$

Dalton Transactions Accepted Manuscript

Summary and graphics for Contents Page

A phosphomide based PNP ligand, 2,6-{$Ph_2PC(O)\}_2(C_5H_3N)$ showing PP, PNP and PNO coordination modes

---

Coordination chemistry of a versatile phosphomide ligand, 2,6-{$Ph_2PC(O)\}_2(C_5H_3N)$ is described.

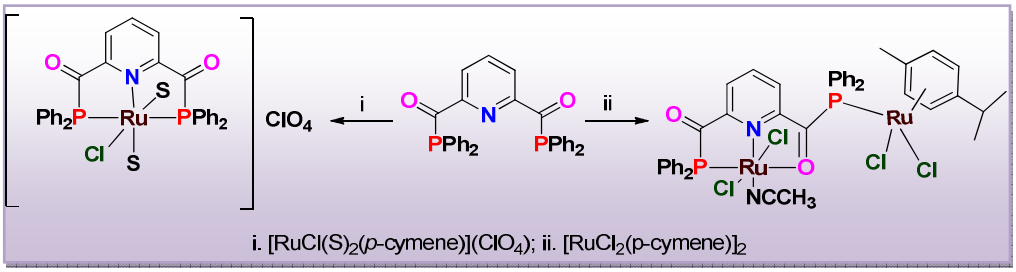

Dalton Transactions Accepted Manuscript